J. Am. Chem. Soc. **1980**, *102*, 7691–7701

Isolation and Structural Characterization of the Triiron Undecacarbonyl Dianion $[Fe_3(CO)_{11}]^{2-}$: Stereochemical Interrelationship with Triiron Dodecacarbonyl and the Triiron Undecacarbonyl Hydride Monoanion

Frederick Yip-Kwai Lo,[1a] Giuliano Longoni,[1b] Paolo Chini,*[1c] Loren D. Lower,[1a] and Lawrence F. Dahl*[1a]

Contribution from the Department of Chemistry, University of Wisconsin—Madison, Madison, Wisconsin 53706, and the Centro del CNR per lo studio e la, sintesi dei composti dei metalli di transizione, and Istituto di Chimica Generale dell' Università, 20133 Milano, Italy.
Received September 12, 1979

Abstract: An X-ray diffraction investigation of the classical $[Fe_3(CO)_{11}]^{2-}$ dianion has finally ascertained its solid-state configuration which represents the heretofore missing structural link between the known triangular iron geometries of the other two closely related and stereochemically prominent triiron carbonyl clusters $Fe_3(CO)_{12}$ and the $[HFe_3(CO)_{11}]^-$ monoanion and of the O-methylated derivative $HFe_3(CO)_{10}(COMe)$ of the monoanion. The $[Fe_3(CO)_{11}]^{2-}$ dianion in the tetraethylammonium salt exemplifies an unprecedented $M_3(CO)_9(\mu\text{-}CO)(\mu_3\text{-}CO)$-type configuration of crystallographic C_s-m symmetry containing a symmetrical doubly bridging carbonyl linking two mirror-related $Fe(CO)_3$ fragments which are connected to each other and to the third $Fe(CO)_3$ fragment by an unsymmetrical triply bridging carbonyl as well as by electron-pair Fe–Fe bonds. A crystallographic examination was first carried out on the tetraphenylarsonium salt, which exhibited for the dianion a centrosymmetric crystal disorder analogous to that previously found for $Fe_3(CO)_{12}$. The resulting overall architecture, unraveled from the superposition of carbonyl peaks for the two centrosymmetrically related, half-weighted orientations, was found to be in accordance with the crystal-ordered configuration of the dianion established from a subsequent structural determination of the tetraethylammonium salt. Salient structural features obtained from the latter, relatively precise analysis include (1) an essentially equilateral iron triangle with two identical Fe_A–Fe_B bonds of 2.593 (2) Å vs. an Fe_B–Fe_B bond of 2.603 (3) Å between the two mirror-related Fe_B atoms, (2) a symmetrically coordinated doubly bridging CO(DB) ligand with two identical Fe_B–CO(DB) distances of 1.96 (1) Å (Evidence is presented for a possible semibridging interaction with the third iron Fe_A even though the observed long Fe_A–CO(DB) distance of 2.72 (1) Å indicates such an interaction to be minimal.), and (3) a triply bridging CO(TB) ligand which is highly unsymmetrical in being 1.85 (1) Å from Fe_A compared to 2.21 (1) Å from both Fe_B atoms. Besides pointing to the insensitivity of the previously reported Mössbauer spectrum of the dianion as the $[Fe(en)_3]^{2+}$ salt in not being able to differentiate between the different environments of the two kinds of iron atoms (viz., Fe_A vs. the two Fe_B), the determined structural parameters for the solid-state configuration of the dianion not only enable an analysis of the existing carbonyl infrared data to be made but also lead to the suggestion of a new kind of possible mechanistic pathway for carbonyl interconversion in solution (involving a synchronous movement of a terminal axial carbonyl on Fe_A and both bridging carbonyls over both triangular faces) in order to account for ^{13}C NMR spectral data exhibiting only one resonance even at low temperatures. This direct axial-to-(face-bridged) pathway is used to rationalize part of the previously observed stereodynamic solution behavior of the $[HFe_3(CO)_{11}]^-$ monoanion and of $Ru_3(CO)_{10}(N_2C_4H_4)$. $[NEt_4]_2^+[Fe_3(CO)_{11}]^{2-}$: fw = 736.15, orthorhombic, *Pcmb* [nonstandard setting of *Pbcm* (D_{2h}^{11}, No. 57)], a = 11.589 (4) Å, b = 14.979 (4) Å, c = 19.527 (5) Å, V = 3389 (2) Å^3, ρ_c = 1.44 g·cm^{-3} for Z = 4. For 1452 diffractometry collected reflections with $I > 2\sigma(I)$, $R_1(F)$ = 6.9% and $R_2(F)$ = 7.8%.

Introduction

Prior to the work presented here, the correct solid-state structure of the $[Fe_3(CO)_{11}]^{2-}$ dianion had not been determined. A knowledge of its static geometry is of particular interest not only in conjunction with its fluxional behavior in solution (vide infra) but also from the viewpoint that its unique geometry consisting of 11 ligands encapsulating a triangular metal core provides a heretofore missing link within the unsubstituted trinuclear iron carbonyl series relative to the crystallographically known geometries of two other members, viz., the neutral $Fe_3(CO)_{12}$ parent[2] and the $[HFe_3(CO)_{11}]^-$ monoanion.[3] These latter triangular iron clusters containing twelve ligands are electronically equivalent to the $[Fe_3(CO)_{11}]^{2-}$ dianion by a formal replacement of a CO or H^- ligand, respectively, with two electrons.

The reddish $[Fe_3(CO)_{11}]^{2-}$ dianion was first isolated in a pure state by Hieber and co-workers[4,5] in 1957 by the reaction of $Fe_3(CO)_{12}$ either with 2 M KOH methanolic solution[4] or with ethylenediamine.[5] Its complex behavior in solution including interconversion to other iron carbonyl anions and carbonyl hydride anions has been further explored by others.[6-10] The diamagnetic character of the $[Fe_3(CO)_{11}]^{2-}$ dianion (as well as that of the protonated $[HFe_3(CO)_{11}]^-$ monoanion) was established[11] from magnetic susceptibility measurements of the $K_2^+[Fe_3(CO)_{11}]^{2-}$ and $[Ni(phen)_3]^{2+}[Fe_3(CO)_{11}]^{2-}$ salts (i.e., the observed paramagnetic moment of 3.3 μ_B for the latter salt was found to be in accordance with the expected moment of 3.2–3.4 μ_B previously reported[12] for the tris(1,10-phenanthroline)nickel(II) dication). On the basis of a preliminary X-ray diffraction analysis (which was presumably coupled with their structural substantiation[13] of

(1) (a) University of Wisconsin-Madison. (b) Centrol del CNR. (c) Istituto di Chimica Generale dell' Università.
(2) (a) Wei, C. H.; Dahl, L. F. *J. Am. Chem. Soc.* **1966**, *88*, 1821–2; **1969**, *91*, 1351–61. (b) Cotton, F. A.; Troup, J. M. *J. Am. Chem. Soc.* **1974**, *96*, 4155–9.
(3) Dahl, L. F.; Blount, J. F. *Inorg. Chem.* **1957**, *4*, 1373–5.
(4) Hieber, W.; Brendel, G. *Z. Anorg. Allg. Chem.* **1957**, *289*, 324–37; 324–37; **1957**, *289*, 338–44.
(5) Hieber, W.; Sedlmeier, J.; Werner, R. *Chem. Ber.* **1957**, *90*, 278–86.
(6) cf.: Calderazzo, F.; Ercoli, R.; Natta, G. In "Organic Syntheses via Metal Carbonyls"; Wender, I., Pino, P., Eds.; Interscience: New York, 1968; Vol. I, pp 1–272, and references cited therein.
(7) Case, J. R.; Whiting, M. C. *J. Chem. Soc.* **1960**, 4632–7.
(8) Hieber, W.; Beutner, H. *Z. Naturforsch., B: Anorg. Chem., Org. Chem., Biochem., Biophys., Biol.* **1962**, *17B*, 211–6.
(9) Hieber, W.; Schubert, E. H. *Z. Anorg. Allg. Chem.* **1965**, *338*, 32–6, 37–46.
(10) Farmery, K.; Kilner, M.; Greatrex, R.; Greenwood, N. N. *J. Chem. Soc. A* **1969**, 2339–45.
(11) Hieber, W.; Floss, J. G. *Z. Anorg. Allg. Chem.* **1957**, *291*, 314–24.
(12) Cf.: Nyholm, R. S. *Q. Rev., Chem. Soc.* **1953**, *7*, 377–406.

0002-7863/80/1502-7691$01.00/0

triply bridging carbonyl ligands for the Fischer–Palm $Ni_3(\eta^5-C_5H_5)_3(\mu_3-CO)_2$ cluster[14]) Mills, Hock, and Robinson[15] in 1959 proposed that the $[Fe_3(CO)_{11}]^{2-}$ dianion is composed of a triangular array of $Fe(CO)_3$ fragments which are coordinated to one another by two triply bridging carbonyl ligands in addition to metal–metal bonds. This molecular model was later found by Greenwood and co-workers[10] to be consistent with their Mössbauer and Nujol mull infrared measurements on $[Fe(en)_3]^{2+}[Fe_3(CO)_{11}]^{2-}$. A room-temperature Mössbauer spectrum exhibited (in addition to a doublet assigned to the cation on the basis of its position being typical for high-spin d^6 Fe(II) complexes) an unbroadened quadrupole doublet which was attributed[10] to the three iron atoms being in equivalent environments. The large observed quadrupole splitting of 2.1 mm/s was ascribed[10] to a highly distorted environment about each iron atom. An IR spectrum in Nujol mull displayed a plethora of ten carbonyl absorption bands ranging from 2089 (w) to 1592 (m) cm^{-1}; this latter frequency was tentatively assigned[10] to the triply bridging carbonyl groups.

Recently, Longoni and Chini[16] synthesized the $[Fe_3(CO)_{11}]^{2-}$ dianion both by previous methods[2,3] as well as by deprotonation[10] of the $[HFe_3(CO)_{11}]^-$ monoanion in a 1.2 N KOH methanolic solution. Salts of this dianion with various counterions including $[NEt_4]^+$, $[PPh_4]^+$, $[AsPh_4]^+$, and $[PPN]^+$ were obtained by metathesis in methanol from the potassium salt. These salts dissolve in THF to give dark red solutions which show infrared absorption bands at 1938 (s), 1910 (ms), 1890 (sh), and 1670 (w, br) cm^{-1}.[17] In Nujol mull the $[PPN]_2{}^+[Fe_3(CO)_{11}]^{2-}$ salt exhibits only one band in the bridging carbonyl region at 1665 cm^{-1}. A ^{13}C NMR investigation by Heaton[18] revealed that the $[Fe_3(CO)_{11}]^{2-}$ dianion is a nonrigid structure in solution in that the ^{13}C spectra exhibit only one sharp singlet at ~231.6 ppm even at low temperatures.

Herein are presented the results of X-ray diffraction studies of both the $[AsPh_4]_2{}^+[Fe_3(CO)_{11}]^{2-}$ and $[NEt_4]_2{}^+[Fe_3(CO)_{11}]^{2-}$ salts. Although the structural characterization of the former salt was impeded by a crystal disorder (of an analogous kind to that previously found[2] for $Fe_3(CO)_{12}$) which thereby precluded an accurate determination of the molecular parameters, a corresponding structural characterization of the latter salt posed no such difficulty. The same overall solid-state configuration was observed together with reasonably precise parameters which have enabled a comparative analysis with other related triangular iron carbonyl complexes including $HFe_3(CO)_{10}(COMe)$.[19] These results have provided a much better understanding of the stereochemistry and bonding of this unusual series of iron clusters.

Experimental Section

$[NEt_4]_2{}^+[Fe_3(CO)_{11}]^{2-}$. (a) Crystal Data. Crystals were grown by slow solvent diffusion from a THF–toluene mixture. A dark brown pentagonal-shaped platelike crystal of thickness of 0.11 mm with perpendicular distances of 0.20–0.28-mm range from the center to the five pentagonal faces was optically chosen and mounted inside a thin-walled Lindemann glass capillary which was evacuated, filled with argon, and then hermetically sealed. After optical alignment of the crystal on a Syntex $P\bar{1}$ diffractometer, 15 diffraction maxima, centered automatically with graphite-monochromatized Mo $K\bar{\alpha}$ radiation ($\lambda(K\alpha_1)$ = 0.709 26 Å; $\lambda(K\alpha_2)$ = 0.713 54 Å), were used to determine the lattice constants and orientation matrix for data collection. Axial photographs showed the Laue symmetry of the crystal to be orthorhombic D_{2h}-mmm. Intensity data were collected via the θ–2θ step scan mode with variable scan speeds ranging from 2.0 to 24.0°/min and with scan widths of 1.0° above $K\alpha_1$ and 1.0° below $K\alpha_2$. A background-to-scan time ratio of 2/3 was made on each side of a peak. The intensities of two standard reflections were periodically measured at intervals of every 98 reflections in order to monitor the instrument's stability as well as the crystal's alignment and decay. No significant changes in the intensities of these standard reflections were observed during the entire data collection over one independent octant of the reciprocal lattice. Intensities were measured at room temperature (~23 °C) between 2θ limits of 3 and 60°, but since the scattering power of the crystal diminished sharply for reflections with $2\theta > 45°$, only the 2566 reflections sampled within the range $3° \leq 2\theta \leq 45°$ were processed. An analytical absorption correction[20a] was applied to the intensity data in that the calculated transmission coefficients (based upon the crystal dimensions and a linear absorption coefficient of 13.6 cm^{-1} for Mo $K\bar{\alpha}$ radiation) varied from 0.577 to 0.862. The indexed faces of the utilized crystal and its perpendicular distance (in mm) from the crystal center to each face are as follows: (010), 0.055; $(0\bar{1}0)$, 0.055; (103), 0.20; $(\bar{1}03)$, 0.24; $(\bar{1}01)$, 0.22; $(\bar{1}0\bar{1})$, 0.28; (100), 0.28. A data reduction[20b,c] gave 1452 independent reflections with $I > 2\sigma(I)$.

The measured lattice constants for the orthorhombic unit cell at 23 °C are a = 11.589 (4) Å, b = 14.979 (4) Å, and c = 19.527 (5) Å. The unit cell volume of 3389 (2) Å^3 and fw of 736.15 g/mol give rise to a calculated density of 1.44 g·cm^{-3} based upon $Z = 4$.

The observed systematic absences of $\{0kl\}$ for l odd and $\{hk0\}$ for k odd indicate the probable space group to be either $Pc2_1b$ or $Pcmb$ [nonstandard settings of $Pca2_1$ (C_{2v}^5, No. 29) and $Pbcm$ (D_{2h}^{11}, No. 57), respectively]. An initial choice of the centrosymmetric space group $Pcmb$ was later substantiated on the basis of the successful structural determination and refinement.

(b) Structural Determination and Refinement. The centrosymmetric space group $P2/c2_1/m2_1/b$ requires that the four dianions in the unit cell lie on fourfold special positions such that one half dianion constitutes the crystallographically independent species. The crystal structure was solved[21,22] via the Patterson interatomic vector method (which yielded initial coordinates for one iron atom) followed by repeated Fourier syntheses[20d] which located 19 other independent nonhydrogen atoms. At this point it was determined that the dianion possesses crystallographic site symmetry C_s-m with 16 independent atoms (of which one iron, three carbon, and three oxygen atoms are situated on the mirror plane). In addition, it was found that four of the eight $[NEt_4]^+$ cations per cell are also positioned on mirror planes and the other four cations are located on twofold axes such that two half cations are crystallographically independent. Least-squares refinement[20e,23] of the determined 20 atoms followed by Fourier and difference Fourier maps resolved the locations

(13) Hock, A. A.; Mills, O. S. In "Advances in the Chemistry of the Coordination Compounds"; Kirschner, S., Ed.; MacMillan: New York, 1961; pp 640–48.

(14) Fischer, E. O.; Palm, C. *Chem. Ber.* **1958**, *91*, 1725–31.

(15) Mills, O. S.; Hock, A. A.; Robinson, G. *Proc. Int. Cong. Pure Appl. Chem.* **1959**, *17*, 143.

(16) Longoni, G.; Chini, P., to be submitted for publication.

(17) It is noteworthy that the three higher frequencies are in excellent agreement with those of 1941 (s), 1913 (m), and 1884 (w) cm^{-1} reported previously for the IR spectrum of the dianion in dimethylformamide solution by Edgell et al. (Edgell, W. F.; Yang, M. T.; Bulkin, B. J.; Bayer, R.; Koizumi, N. *J. Am. Chem. Soc.* **1965**, *87*, 3080–8).

(18) Heaton, B. T., personal communication to P. Chini, 1977.

(19) Shriver, D. F.; Lehman, D.; Strope, D. *J. Am. Chem. Soc.* **1975**, *97*, 1594–6.

(20) (a) Blount, J. F. "DEAR, a FORTRAN Absorption-Correction Program", 1965, based on the method given by: Busing, W. R.; Levy, H. A. *Acta Crystallogr.* **1957**, *10*, 180–2. (b) Broach, R. W. "CARESS, a FORTRAN Program for the Computer Analysis of Step-Scan Data", Ph.D. Thesis, University of Wisconsin—Madison, 1977, Appendix I. (c) Broach, R. W. "QUICKSAM, a FORTRAN Program for Sorting and Merging Structure Factor Data", Ph.D. Thesis, University of Wisconsin—Madison, 1977, Appendix II. (d) Calabrese, J. C. "MAP, a FORTRAN Summation and Molecular Assemblage Program", University of Wisconsin—Madison, 1972. (e) Calabrese, J. C. "A Crystallographic Variable Matrix Least-Squares Refinement Program", University of Wisconsin—Madison, 1972. (f) Calabrese, J. C. "MIRAGE", Ph.D. Thesis, University of Wisconsin—Madison, 1971, Appendix III. (g) Busing, W. R.; Martin, K. O.; Levy, H. A. "OR FLS, A FORTRAN Crystallographic Least-Squares Program", Report ORNL-TM-305, Oak Ridge National Laboratory, Oak Ridge, Tennessee, 1962. (h) Busing, W. R.; Martin, K. O.; Levy, H. A. "OR FFE, A FORTRAN Crystallographic Function and Error Program", Report ORNL-TM-306, Oak Ridge National Laboratory, Oak Ridge, Tennessee, 1964. (i) Smith, D. L. "PLANES" Ph.D. Thesis, University of Wisconsin—Madison, 1962, Appendix IV. (j) Johnson, C. K. "OR TEP-II, A FORTRAN Thermal-Ellipsoid Plot Program for Crystal Structure Illustrations", Report ORNL-5138, Oak Ridge National Laboratory, Oak Ridge, Tennessee, 1976. (k) "OR FLSR, A Local Rigid-Body Least-Squares Program", adapted from the Busing–Martin–Levy OR FLS.

(21) Atomic scattering factors for neutral atoms were used.[22a,b] Anomalous dispersion corrections[22c] were applied to the scattering factors of the Fe and As atoms in the structural determinations of the $[AsPh_4]^+$ and $[NEt_4]^+$ salts.

(22) (a) Cromer, D. T.; Mann, J. B. *Acta Crystallogr., Sect. A* **1968**, *A24*, 321–4. (b) Stewart, R. F.; Davidson, E. R.; Simpson, W. T. *J. Chem. Phys.* **1965**, *42*, 3175–87. (c) "International Tables for X-Ray Crystallography", Kynoch Press: Birmingham, England, 1974; Vol. IV, p 149.

(23) The unweighted and weighted discrepancy factors used are $R_1(F) = 100[\sum||F_o| - |F_c||/\sum|F_o|]$ and $R_2(F) = 100[\sum w_i||F_o| - |F_c||^2/\sum w_i|F_o|^2]^{1/2}$. All least-squares refinements were based on the minimization of $\sum w_i||F_o| - |F_c||^2$ with individual weights of $w_i = 1/\sigma^2(F_o)$.

Table I. Atomic Parameters for $[NEt_4]_2^+[Fe_3(CO)_{11}]^{2-}$

A. Positional Parameters[a]

atom	x	y	z
Fe(1)	0.35673 (16)	3/4	0.48284 (9)
Fe(2)	0.18246 (11)	0.66311 (10)	0.43296 (7)
C(1)	0.2120 (12)	3/4	0.5229 (7)
O(1)	0.1636 (8)	3/4	0.5779 (5)
C(2)	0.2336 (11)	3/4	0.3641 (7)
O(2)	0.2693 (9)	3/4	0.3075 (5)
C(3)	0.4608 (12)	3/4	0.4144 (7)
O(3)	0.5333 (9)	3/4	0.3750 (5)
C(4)	0.4060 (10)	0.6600 (13)	0.5296 (6)
O(4)	0.4397 (9)	0.5996 (11)	0.5635 (6)
C(5)	0.0580 (13)	0.6438 (9)	0.3842 (7)
O(5)	−0.0271 (10)	0.6360 (10)	0.3535 (6)
C(6)	0.2808 (12)	0.5889 (8)	0.3995 (7)
O(6)	0.3499 (11)	0.5395 (7)	0.3775 (5)
C(7)	0.1302 (10)	0.5974 (8)	0.5026 (6)
O(7)	0.0980 (8)	0.5503 (6)	0.5467 (4)
N(1)	0.2024 (9)	1/4	0.4163 (6)
C(11)	0.2471 (18)	0.1924 (15)	0.3557 (11)
C(12)	0.1030 (19)	0.1827 (29)	0.3863 (19)
C(13)	0.3044 (16)	0.3101 (14)	0.4416 (12)
C(14)	0.1589 (23)	0.3089 (25)	0.4799 (13)
C(15)	0.1502 (15)	0.1321 (12)	0.3248 (9)
C(16)	0.2676 (16)	0.3680 (9)	0.5063 (7)
N(2)	0.3305 (8)	1/2	3/4
C(21)	0.2604 (10)	0.5378 (9)	0.6944 (5)
C(22)	0.4041 (12)	0.4312 (9)	0.7177 (6)
C(23)	0.1784 (25)	0.6056 (17)	0.7112 (7)
C(24)	0.4974 (16)	0.3920 (13)	0.7623 (8)
H(21-1)[b]	0.221	0.489	0.669
H(21-2)	0.312	0.560	0.657
H(22-1)	0.438	0.455	0.675
H(22-2)	0.354	0.381	0.700
H(23-1)	0.137	0.625	0.669
H(23-2)	0.219	0.658	0.732
H(23-3)	0.121	0.581	0.745
H(24-1)	0.542	0.347	0.735
H(24-2)	0.464	0.364	0.804
H(24-3)	0.552	0.442	0.777

B. Anisotropic Thermal Parameters ($\times 10^4$)[c]

atom	β_{11}	β_{22}	β_{33}	β_{12}	β_{13}	β_{23}
Fe(1)	61 (2)	107 (2)	20 (1)	0	0 (1)	0
Fe(2)	83 (1)	50 (1)	30 (0)	1 (1)	2 (1)	−1 (1)
C(1)	91 (14)	112 (13)	16 (4)	0	13 (6)	0
O(1)	86 (9)	108 (8)	29 (3)	0	5 (4)	0
C(2)	91 (13)	61 (9)	23 (4)	0	−12 (6)	0
O(2)	155 (12)	96 (8)	19 (3)	0	7 (5)	0
C(3)	73 (13)	74 (11)	31 (5)	0	−3 (7)	0
O(3)	108 (10)	93 (8)	33 (3)	0	25 (5)	0
C(4)	87 (11)	242 (18)	33 (4)	13 (12)	14 (6)	39 (7)
O(4)	173 (12)	309 (17)	79 (5)	54 (11)	16 (7)	114 (8)
C(5)	185 (17)	111 (12)	52 (5)	−71 (11)	−13 (8)	16 (6)
O(5)	239 (16)	299 (17)	86 (5)	−156 (14)	−77 (8)	27 (8)
C(6)	202 (17)	62 (8)	52 (5)	17 (10)	52 (8)	7 (5)
O(6)	338 (18)	101 (7)	83 (5)	67 (10)	93 (8)	4 (5)
C(7)	130 (12)	63 (8)	45 (5)	27 (8)	20 (6)	0 (5)
O(7)	211 (12)	81 (6)	59 (3)	20 (7)	46 (5)	24 (4)
N(1)	64 (11)	121 (11)	45 (5)	0	11 (6)	0
C(11)	111 (21)	94 (16)	45 (8)	−21 (16)	17 (11)	−35 (10)
C(12)	57 (20)	300 (50)	97 (16)	−112 (25)	−7 (15)	61 (23)
C(13)	83 (18)	68 (13)	51 (9)	−7 (13)	−2 (10)	−11 (9)
C(14)	138 (27)	272 (48)	47 (10)	160 (30)	33 (14)	12 (15)
C(15)	232 (22)	148 (15)	62 (6)	−100 (15)	−27 (10)	−5 (8)
C(16)	291 (25)	85 (10)	55 (5)	67 (13)	−1 (10)	−23 (6)
N(2)	73 (9)	60 (7)	27 (3)	0	0	−6 (4)
C(21)	140 (12)	102 (10)	31 (3)	14 (10)	10 (6)	18 (5)
C(22)	199 (17)	104 (10)	38 (4)	43 (11)	−33 (7)	−32 (5)
C(23)	666 (53)	254 (24)	38 (5)	298 (31)	28 (13)	36 (9)
C(24)	350 (27)	235 (19)	67 (6)	223 (20)	−66 (12)	−87 (10)

[a] The seven Fe(1), C(n), and O(n) atoms (n = 1–3) in the independent half dianion and the N(1) atom in one of the two independent half $[NEt_4]^+$ cations each occupy a set of fourfold special positions (4d) on a mirror plane: $\pm(x, {}^1/_4, z; x, {}^3/_4, {}^1/_2 - z)$. Likewise, the N(2) atoms in the other independent half $[NEt_4]^+$ cation occupies a set of fourfold special positions (4c) on a twofold axis: $\pm(x, 0, {}^1/_4; x, {}^1/_2, {}^1/_4)$. Each of the other independent atoms occupies an eightfold set (8e) of general positions: $\pm(x, y, z; x, y, {}^1/_2 + z; x, {}^1/_2 - y, z; x, {}^1/_2 + y, {}^1/_2 - z)$. These latter independent atoms include: (1) nine Fe(2), C(n), and O(n) atoms (n = 4–7) in half of the dianion; (2) four half-weighted methylene C(1n) atoms (n = 1–4) and two whole-weighted methyl C(15) and C(16) atoms (each due to an assumed superposition of two half-weighted methyl carbon sites) in the mirror-constrained half $[NEt_4]^+$ cation; and (3) two methylene C(21) and C(22) atoms, two methyl C(23) and C(24) atoms, four methylene H(21-n) and H(22-n) atoms (n = 1, 2), and six methyl H(23-n) and H(24-n) atoms (n = 1–3) in the twofold-constrained half $[NEt_4]^+$ cation. No idealized hydrogen positions were obtained for the crystal-disordered mirror-constrained $[NEt_4]^+$ cation. [b] Idealized coordinates for the methylene and methyl hydrogen atoms of the ordered tetraethylammonium cation were calculated on the basis of an assumed regular staggered tetrahedral geometry with C–H distances of 1.0 Å. These hydrogen positions (which were calculated after each cycle of least squares due to their dependence upon the shifted carbon positions) together with an assumed individual isotropic temperature factor of 6.0 Å^2 were included in the least-squares refinement as fixed-atom contributions. [c] The anisotropic thermal parameters are of the form $\exp[-(h^2\beta_{11} + k^2\beta_{22} + l^2\beta_{33} + 2hk\beta_{12} + 2hl\beta_{13} + 2kl\beta_{23})]$.

of the other nonhydrogen atoms. These maps revealed that each of the four methylene carbon atoms in the mirror-constrained $[NEt_4]^+$ cation is randomly disordered between two tetrahedral sites with each of the four methyl carbon atoms being ordered (due to presumed superimposed positioning). Hence, each of the four independent methylene carbon sites was given an occupancy factor of $^1/_2$. An isotropic least-squares refinement converged at $R_1(F)$ = 14.1% and $R_2(F)$ = 15.6%.[23] Idealized tetrahedral coordinates for the hydrogen atoms in the ordered half $[NEt_4]^+$ cation were calculated[20f] at that time. Further least-squares refinement[20g] was then carried out with varying positional and anisotropic thermal parameters for the nonhydrogen atoms and with fixed positional and fixed isotropic temperature parameters for the hydrogen atoms. After each cycle of refinement, new regular tetrahedral coordinates for each hydrogen atom were calculated on the basis of the new carbon positions. The final cycle of the full-matrix least-squares refinement converged to $R_1(F)$ = 6.9% and $R_2(F)$ = 7.8% with no parameter shift-to-error ratio being greater than 0.06. The standard error-of-fit was 1.79, while the data-to-parameter ratio was 6.5/1. A final difference map revealed no unusual features.

The atomic parameters from the output of the final least-squares cycle are given in Table I. Interatomic distances and bond angles[20b] are presented in Table II and selected least-squares planes[20i] and interplanar angles in Table III. Observed and calculated structure factors are tabulated as supplementary material. All figures were computer-generated and computer-drawn.[20j]

$[AsPh_4]_2^+[Fe_3(CO)_{11}]^{2-}$. (a) Crystal Data. Crystals suitable for X-ray investigation were obtained via an acetone–isopropyl alcohol solvent diffusion. A cylindrical-shaped needle-like crystal of 0.22-mm diameter and 0.42-mm length was selected by optical examination. The procedures for crystal alignment and data collection were analogous to those previously described for the tetraethylammonium salt. Axial photographs confirmed both the lattice lengths and symmetry of the chosen monoclinic unit cell. The intensities of 3863 reflections were measured for the reciprocal lattice octants hkl and $\bar{h}kl$ over the range 3° ≤ 2θ ≤ 45°. A linear decay correction of ~5% (based upon the variations in intensities of two standard reflections) was applied to the intensities. A sorting and merging of the reduced data gave 3724 independent reflections, of which 1816 had diffraction maxima greater than $2\sigma(I)$. An absorption correction was made (on the basis of the linear absorption coefficient of 21.7 cm^{-1} for Mo K$\bar{\alpha}$ radiation).

The determined monoclinic cell constants at 23 °C are a = 17.894 (3) Å, b = 10.285 (2) Å, c = 14.835 (2) Å, β = 99.21 (1)°, and V = 2695

Table II. Interatomic Distances and Bond Angles for $[NEt_4]_2{}^+[Fe_3(CO)_{11}]^{2-}$

A. Intraanion Distances (Å)[a]

Fe(1)–Fe(2)	2.593 (2)	C(5)–O(5)	1.161 (14)
Fe(2)–Fe(2′)	2.603 (3)	C(6)–O(6)	1.171 (13)
Fe(1)–C(1)	1.850 (13)	C(7)–O(7)	1.175 (12)
Fe(1)···C(2)	2.723 (13)	C(1)···C(4)	2.624 (18)
Fe(1)–C(3)	1.800 (15)	C(1)···C(7)	2.506 (14)
Fe(1)–C(4)	1.725 (17)	C(2)···C(3)	2.809 (18)
Fe(2)–C(1)	2.212 (11)	C(2)···C(5)	2.612 (17)
Fe(2)–C(2)	1.963 (11)	C(2)···C(6)	2.569 (13)
Fe(2)–C(5)	1.752 (15)	C(3)···C(4)	2.698 (18)
Fe(2)–C(6)	1.721 (13)	C(3)···C(6)	3.203 (15)
Fe(2)–C(7)	1.784 (13)	C(4)···C(4′)	2.696 (39)
C(1)–O(1)	1.212 (14)	C(5)···C(5′)	3.180 (28)
C(2)–O(2)	1.180 (14)	C(5)···C(6)	2.726 (21)
C(3)–O(3)	1.140 (14)	C(6)···C(7)	2.667 (16)
C(4)–O(4)	1.186 (17)		

B. Intraanion Bond Angles (Deg)[a]

Fe(2)–Fe(1)–Fe(2′)	60.27 (8)	C(1)–Fe(1)–C(3)	157.0 (6)
Fe(1)–Fe(2)–Fe(2′)	59.87 (4)	C(1)–Fe(1)–C(4)	94.4 (4)
C(1)–Fe(1)–Fe(2)	56.8 (3)	C(3)–Fe(1)–C(4)	99.9 (5)
C(1)–Fe(2)–Fe(1)	44.4 (3)	C(4)–Fe(1)–C(4′)	102.8 (4)
C(1)–Fe(2)–Fe(2′)	54.0 (2)	C(1)–Fe(2)–C(2)	96.1 (4)
C(2)–Fe(2)–Fe(1)	71.9 (3)	C(1)–Fe(2)–C(5)	131.0 (6)
C(2)–Fe(2)–Fe(2′)	48.5 (3)	C(1)–Fe(2)–C(6)	125.4 (6)
C(3)–Fe(1)–Fe(2)	104.1 (4)	C(1)–Fe(2)–C(7)	76.8 (4)
C(4)–Fe(1)–Fe(2)	93.7 (5)	C(2)–Fe(2)–C(5)	89.2 (5)
C(4)–Fe(1)–Fe(2′)	148.1 (4)	C(2)–Fe(2)–C(6)	88.2 (5)
C(5)–Fe(2)–Fe(1)	158.1 (4)	C(2)–Fe(2)–C(7)	171.9 (4)
C(5)–Fe(2)–Fe(2′)	99.5 (5)	C(5)–Fe(2)–C(6)	103.4 (7)
C(6)–Fe(2)–Fe(1)	87.2 (5)	C(5)–Fe(2)–C(7)	92.5 (6)
C(6)–Fe(2)–Fe(2′)	130.2 (4)	C(6)–Fe(2)–C(7)	99.1 (5)
C(7)–Fe(2)–Fe(1)	104.8 (4)	Fe(1)–C(1)–O(1)	142.6 (11)
C(7)–Fe(2)–Fe(2′)	123.5 (3)	Fe(2)–C(1)–O(1)	129.2 (7)
Fe(1)–C(1)–Fe(2)	78.8 (4)	Fe(2)–C(2)–O(2)	138.4 (3)
Fe(2)–C(1)–Fe(2′)	72.1 (4)	Fe(1)–C(3)–O(3)	174.5 (12)
Fe(2)–C(2)–Fe(2′)	83.1 (6)	Fe(1)–C(4)–O(4)	178.0 (15)
		Fe(2)–C(5)–O(5)	175.8 (16)
		Fe(2)–C(6)–O(6)	178.3 (14)
		Fe(2)–C(7)–O(7)	176.5 (10)

C. Distances (Å) and Bond Angles (Deg) for Two Tetraethylammonium Cations[a]

N(1)–C(11)	1.55 (2)	C(11)–C(15)	1.56 (2)
N(1)–C(12)	1.64 (3)	C(12)–C(15)	1.52 (4)
N(1)–C(13)	1.57 (2)	C(13)–C(16)	1.59 (2)
N(1)–C(14)	1.60 (3)	C(14)–C(16)	1.62 (4)
N(2)–C(21)	1.47 (1)	C(21)–C(23)	1.43 (2)
N(2)–C(22)	1.48 (1)	C(22)–C(24)	1.51 (2)
C(11)–N(1)–C(13)	108 (1)	C(21)–N(2)–C(22)	105.8 (6)
C(11)–N(1)–C(12′)	108 (2)	C(21)–N(2)–C(21″)	112.9 (11)
C(11)–N(1)–C(14′)	113 (1)	C(21)–N(2)–C(22″)	111.4 (8)
C(13)–N(1)–C(12′)	107 (2)	C(22)–N(2)–C(22″)	109.5 (12)
C(13)–N(1)–C(14′)	108 (1)	N(2)–C(21)–C(23)	118.1 (10)
C(12′)–N(1)–C(14′)	113 (2)	N(2)–C(22)–C(24)	116.1 (8)
N(1)–C(11)–C(15)	112 (2)		
N(1)–C(12′)–C(15′)	110 (2)		
N(1)–C(13)–C(16)	111 (1)		
N(1)–C(14′)–C(16′)	108 (1)		

[a] The single primed numbers are those related by a crystallographic mirror plane, while the double primed distances are those related by a crystallographic twofold axis.

Å³. On the basis of a fw of 1242.4 g/mol, the calculated density of 1.53 $g \cdot cm^{-3}$ for $Z = 2$ is identical with the experimental value of 1.53 ± 0.03 $g \cdot cm^{-3}$ obtained by the flotation method with CCl_4–$CHCl_3$ mixtures.

Systematic absences of $\{h0l\}$ for $h + l$ odd and $\{0k0\}$ for k odd uniquely define the probable space group to be $P2_1/n$ [related by an alternative unit cell to $P2_1/c$ (C_{2h}^5, No. 14)].

(b) Structural Determination and Refinement. The centrosymmetric space group crystallographically demands that each of the two $[Fe_3(CO)_{11}]^{2-}$ dianions per cell possesses a centrosymmetric crystal disorder in which each dianion assumes a random distribution in one of two orientations related to each other by a center of symmetry. Hence, the solution of the crystal structure involved the determination of the coordinates of three half-weighted iron atoms and eleven half-weighted carbonyl ligands along with the atomic coordinates for one independent tetraphenylarsonium cation.

Table III. Least-Squares Planes for the $[Fe_3(CO)_{11}]^{2-}$ Dianion

A. Planes and Perpendicular Distances (Å) of Selected Atoms from These Planes[a]

1. Plane through Fe(1), Fe(2), Fe(2′)

$0.4344X - 0.9007Z + 6.6962 = 0$

C(1)	−1.43	C(5)	0.23
C(2)	1.47	C(6)	1.08
C(3)	1.73	C(7)	−1.49
C(4)	−0.57		

2. Plane through Fe(1), C(4), C(4′)

$0.8480X - 0.5300Z + 1.4908 = 0$

O(4)	−0.02

3. Plane through Fe(2), Fe(2′), C(1)

$0.9815X - 0.1914Z - 0.4574 = 0$

Fe(1)	1.80	C(4′)	2.18
O(1)	−0.76	C(6)	1.24
C(4)	2.18	O(6)	2.11

4. Plane through Fe(2), Fe(2′), C(2)

$-0.9150X - 0.4034Z + 5.3454 = 0$

O(2)	0.07	C(7)	0.01
C(6)	−0.78	O(7)	0.00
O(6)	−1.34		

B. Angles (Deg) between Normals to Planes

plane	angle	plane	angle
1–2	32.2	2–3	159.0
1–3	53.2	3–4	145.2
1–4	92.0		

[a] The equations of the planes are given in an angstrom orthogonal coordinate system (X, Y, Z), which is related to the orthorhombic crystallographic fractional coordinates (x, y, z) by the transformations: $X = ax$, $Y = by$, and $Z = cz$. Unit weights were used in the calculations of the planes.

An analysis of a three-dimensional Patterson function yielded initial positions for the arsenic and three half-weighted iron atoms. Successive Fourier syntheses followed by rigid-body least-squares refinement[20k] (with varying individual isotropic temperature factors), in which the four phenyl rings were each constrained to their well-known geometry, provided reasonably precise atomic parameters for the tetraphenylarsonium cation. Fourier difference maps were then utilized in attemps to unravel the superposition of peaks arising from the two half-weighted orientations of the dianion. Although the crystal structure of the $[NEt_4]_2{}^+[Fe_3(CO)_{11}]^{2-}$ salt had not been characterized at that time, it was presumed that the static configuration of the dianion should be related to those then known for $Fe_3(CO)_{12}$ and the $[HFe_3(CO)_{11}]^-$ monoanion. An averaged statistical structure was thereby deduced from the observed peaks consistent with three terminal carbonyl ligands being coordinated to each Fe atom and with one doubly bridging carbonyl and one triply bridging carbonyl. Least-squares refinement of both isotropic and anisotropic thermal models gave $R_1(F)$ values as low as 14%.[24] However, the relatively large uncertainties in the positional parameters of the carbonyl ligands due to the crystal disorder does not make physically meaningful any detailed analysis of individual carbonyl ligands in terms of bond lengths and angles. Nevertheless, the overall averaged disordered geometry (previously communicated[25]) derived for the $[Fe_3(CO)_{11}]^{2-}$ dianion in the $[AsPh_4]^+$ salt is in complete accordance with the detailed geometry reported here for the $[NEt_4]^+$ salt.

Results and Discussion

General Description of the Crystal Structure of $[NEt_4]_2{}^+[Fe_3(CO)_{11}]^{2-}$. The crystalline arrangement of the four dianions and

(24) The determined Fe–Fe distances reflect the inherently large error in molecular parameters associated with this averaged disordered structure which is assumed to conform ideally to C_s-m symmetry. The two Fe–Fe distances for the chemically equivalent bonds are 2.53 and 2.58 Å; the Fe–Fe distance between the two equivalent iron atoms connected by the doubly bridging carbonyl is 2.62 Å. These values are in reasonable agreement with the Fe–Fe bond lengths obtained for the structure of $[NEt_4]_2{}^+[Fe_3(CO)_{11}]^{2-}$.

(25) Lower, L. D.; Dahl, L. F.; Longoni, G.; Chini, P. "Abstracts of Papers", 170th National Meeting of the American Chemical Society, Chicago, Illinois, 1975; American Chemical Society: Washington, D.C., 1975; INOR 68.

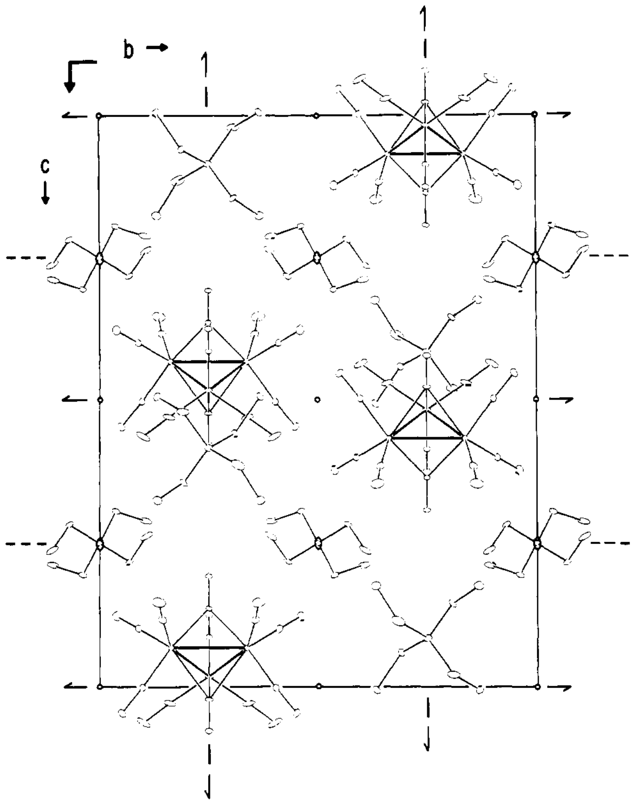

Figure 1. View depicting the orientations of the eight tetraethylammonium cations and four $[Fe_3(CO)_{11}]^{2-}$ dianions in the orthorhombic unit cell of centrosymmetric space group symmetry $P2/c2_1/m2_1/b$. Each of the four *ordered*, equivalent dianions lies on a mirror plane passing through one iron and three carbonyl ligands. Of the eight $[NEt_4]^+$ cations per cell, each of four equivalent ones is located in an *ordered* manner about a twofold axis. A composite of two orientations of each of the other four *disordered* cations lies on a mirror plane such that each of the four methylene carbon atoms is randomly disordered between two tetrahedral sites, while each of the four methyl carbon atoms is ordered due to presumed superimposed positioning. Only one of the two orientations of each of the four crystal-disordered cations is shown.

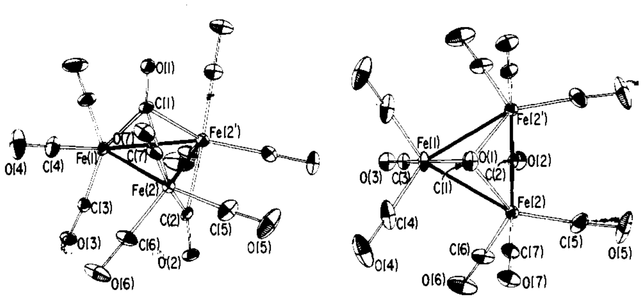

Figure 2. Two views of the crystal-ordered $[Fe_3(CO)_{11}]^{2-}$ dianion of crystallographic C_s-m site symmetry in the tetraethylammonium salt.

eight tetraethylammonium cations in the orthorhombic unit cell (Figure 1) gives rise to each dianion possessing crystallographic site symmetry C_s-m. The four cations which lie on crystallographic C_2-2 axes are ordered in contrast to the other four cations which lie on crystallographic mirror planes being randomly disordered between two orientations. There are no unusual interionic contacts with both the shortest C(methyl)···OC and C(methylene)···OC separations being 3.3 Å.

Structural Features of the $[Fe_3(CO)_{11}]^{2-}$ Dianion. Its configuration (Figure 2) of bilateral symmetry consists of a completely bonding triangular array of iron atoms containing an $Fe(CO)_3$ group which is symmetrically linked to both mirror-related iron atoms in a $Fe_2(CO)_6(\mu\text{-}CO)$ fragment by a triply bridging carbonyl ligand as well as by electron-pair Fe–Fe bonds. An examination of the distances and bond angles provides further insight concerning the mode of carbonyl environment about the triangular

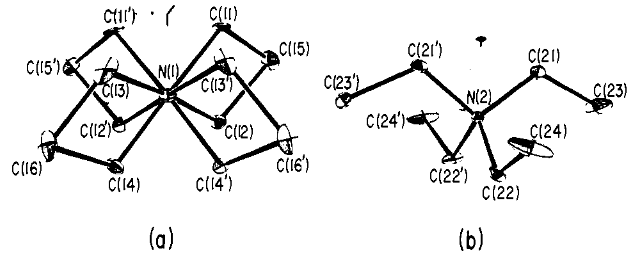

Figure 3. Views of (a) the composite of two equally probable orientations of a crystal-*disordered* tetraethylammonium cation located on a crystallographic mirror plane passing through N(1) and (b) the configuration of a crystal-*ordered* tetraethylammonium cation located on a crystallographic twofold axis passing through N(2). The particular mirror-plane crystal disorder of a $[NEt_4]^+$ cation produces a cube of eight half-weighted methylene carbon atoms but only four whole-weighted methyl carbon atoms due to the latter positions representing the average of the assumed identical positions for the two equally weighted orientations.

iron core. The iron triangle is virtually equilateral with the two identical Fe(1)–Fe(2) bonds of 2.593 (2) Å being essentially equivalent to the third Fe(2)–Fe(2′) bond of 2.603 (3) Å between the two mirror-related iron atoms. The observed variations in the Fe–CO bond lengths for the five independent carbonyl ligands conform to qualitative bonding expectations (based upon the influence of the trans ligand), even though the bond length differences are on the borderline of statistical significance. The Fe(1)–C(3) bond which is trans to the relatively short Fe(1)–C-(triply bridged) bond has the longest distance of 1.800 (15) Å, while the Fe(2)–C(7) bond which is trans to the Fe(2)–C(doubly bridged) bond has the next longest distance of 1.784 (13) Å. The other three shorter Fe–CO bonds of range 1.721 (13)–1.752 (15) Å may each be regarded as being trans to electron-pair Fe–Fe bonds.

The doubly bridging carbonyl ligand lying on the mirror plane is symmetrically coordinated to the two equivalent iron atoms with identical Fe(2)–C(2) and Fe(2′)–C(2) distances of 1.963 (11) Å. Its essentially nonbonding interaction (vide infra) with the third iron atom is indicated by a long Fe(1)···C(2) distance of 2.723 (13) Å. The C(2)–O(2) bond length of 1.180 (14) Å and the Fe(2)–C(2)–Fe(2′) bond angle of 83.1 (6)° are also within the normal ranges for doubly bridging carbonyl ligands.

The triply bridging carbonyl ligand, which is also situated on the mirror plane, is asymmetrically coordinated to the three iron atoms, being only 1.850 (13) Å from the unique Fe(1) atom vs. being 2.212 (11) Å from each of the two equivalent Fe(2) and Fe(2′) atoms. This considerable bond length asymmetry is also reflected in the Fe(1)–C(1)–Fe(2) bond angle of 78.8 (4)° being markedly larger than the Fe(2)–C(1)–Fe(2′) bond angle of 72.1 (4)°. The longer C(1)–O(1) bond length of 1.212 (14) Å is within the expected range of values for triply bridging carbonyl ligands.

Structural Features of the Tetraethylammonium Cations. One of the four equivalent mirror-disordered tetraethylammonium cations per cell is shown in Figure 3a. It is apparent that the mirror plane passing only through N(1) produces a random distribution of the cation in one of two orientations in the crystal with a disordering of the four tetrahedrally disposed methylene carbon atoms but with an indicated ordering of each of the four methyl carbon atoms due to an assumed superimposed positioning of the corresponding half-weighted methyl sites (which were not resolved on Fourier maps). The resulting crystal disorder may be structurally viewed as a cube of eight half-weighted methylene carbon atoms (encapsulating N(1)) arising from two interpenetrating carbon tetrahedra which are related to each other by the crystallographic mirror plane. Table II shows (in light of the crystal disorder) that all distances and bond angles are reasonable values. A disordering of tetraethylammonium cations in the crystalline state is not uncommon.[26]

(26) Cf.: Handy, L. B.; Ruff, J. K.; Dahl, L. F. *J. Am. Chem. Soc.* **1970**, *92*, 7312–26. Roziere, J.; Williams, J. M.; Stewart, Jr., R. P.; Peterson, J. L.; Dahl, L. F. *Ibid.* **1977**, *99*, 4497–9.

Of the other four tetraethylammonium cations per cell located on crystallographic twofold axes (Figure 1) it is clear from Figure 3b, which depicts the configuration of one of these equivalent cations, that its entire architecture is ordered. Likewise, all bond length and bond angle values (Table II) are normal.

Although it is conceivable that the crystal disorder of the mirror-constrained tetraethylammonium cations may arise from the use of the centrosymmetric space group *Pcmb* instead of the corresponding noncentrosymmetric one $Pc2_1b$ (which removes the mirror plane passing through N(1)), this latter possibility was deemed highly unlikely and therefore not pursued. Our judgment that the unit cell possesses centrosymmetric *Pcmb* symmetry is based upon (1) the intensity data closely conforming to a centrosymmetric intensity distribution, (2) the crystal structure refinement under *Pcmb* being entirely satisfactory with no unusual distances or bond angles reflecting an incorrect choice of this space group which also imposes a mirror plane constraint on the crystal-ordered dianions and a twofold constraint on the other crystal-ordered tetraethylammonium cations, and (3) an analysis of the sizes, shapes, and orientations of the atomic thermal ellipsoids providing no evidence for any anomalous features which would be caused by a wrong space group assignment.

Correlation of the $Fe_3(CO)_9(\mu\text{-}X)(\mu_3\text{-}Y)$ Type Structure for the $[Fe_3(CO)_{11}]^{2-}$ Dianion with the $Fe_3(CO)_9(\mu_3\text{-}X)(\mu_3\text{-}Y)$ Type Structure for the Electronically Equivalent $Fe_3(CO)_9(\mu_3\text{-}As)_2$ and $Fe_3(CO)_9(\mu_3\text{-}CO)(\mu_3\text{-}NSiMe_3)$ Molecules Which Likewise Contain Eleven Ligands Coordinated to a Completely Bonding Iron Triangle. To our knowledge the solid-state configuration of the $[Fe_3(CO)_{11}]^{2-}$ dianion provides the first example of a $M_3(CO)_9(\mu\text{-}X)(\mu_3\text{-}Y)$ type complex (where X = Y = CO), possessing a completely bonding metal triangle with one doubly bridging X ligand and one triply bridging Y ligand. The $Fe_3(CO)_9(\mu_3\text{-}X)(\mu_3\text{-}Y)$ type model (with both triply bridging X and Y ligands) proposed by Mills and co-workers[15] and accepted by others[10] for the $[Fe_3(CO)_{11}]^{2-}$ dianion has been subsequently uncovered for two structurally resembling iron molecules, $Fe_3(CO)_9(\mu_3\text{-}As)_2$[27] and $Fe_3(CO)_9(\mu_3\text{-}CO)(\mu_3\text{-}NSiMe_3)$,[28] containing completely bonding iron triangles such that the neutral molecules are thereby electronically equivalent to the $[Fe_3(CO)_9(\mu\text{-}CO)(\mu_3\text{-}CO)]^{2-}$ dianion. The molecular parameters of both $Fe_3(CO)_9(\mu_3\text{-}As)_2$ and $Fe_3(CO)_9(\mu_3\text{-}CO)(\mu_3\text{-}NSiMe_3)$ ideally exhibit an equilateral triangle of iron atoms with the triply bridging ligands symmetrically adjoined. In the case of the $Fe_3(CO)_9(\mu_3\text{-}As)_2$ molecule (for which the crystal structure is disordered with each molecule randomly distributed in two orientations related by a crystallographic twofold axis), its geometry approximately conforms to C_{3h}-$\bar{3}/m$ with one terminal carbonyl of each $Fe(CO)_3$ fragment located on the horizontal mirror and the other two terminal carbonyls related by this mirror plane.[27] In the case of the $Fe_3(CO)_9(\mu_3\text{-}CO)(\mu_3\text{-}NSiMe_3)$ molecule which possesses a pseudo-threefold geometry,[28] the three $Fe(CO)_3$ fragments are similarly oriented (except for a slight twisting due presumably to steric interactions) to those in the $Fe_3(CO)_9(\mu_3\text{-}As)_2$ molecule. The average Fe–Fe bond lengths of 2.62 (1) Å in $Fe_3(CO)_9(\mu_3\text{-}As)_2$ and 2.535 (2) Å in $Fe_3(Co)_9(\mu_3\text{-}CO)(\mu_3\text{-}NSiMe_3)$ are in accord with a closed-shell krypton-like configuration being achieved for each iron atom by formation of three electron-pair Fe–Fe bonds corresponding in MO language to the bonding in-plane a_1 + e trimetal symmetry orbitals (SO's) being filled and the corresponding antibonding in-plane a_1^* + e* trimetal SO's (under C_{3v} symmetry) being empty.

The observed conformity of the $[Fe_3(CO)_{11}]^{2-}$ dianion to the $Fe_3(CO)_9(\mu\text{-}X)(\mu_3\text{-}Y)$ type structure instead of the $Fe_3(CO)_9(\mu_3\text{-}X)(\mu_3\text{-}Y)$ type structure (i.e., in this case of a completely bonding metal triangle, both structures are valence bond isomers of each other[29-31]) may be rationalized on the basis of electronic effects with a dominant factor being a presumed lack of enough charge density on Fe(1) in order that sufficiently large π^*(CO) back-bonding can occur to render stable a geometry with two triply bridging carbonyl ligands. This premise is to a considerable extent based on a detailed structural bonding analysis[32,33] of two (triangular metal)-bonding $Rh_3(\eta^5\text{-}C_5H_5)_3(CO)(RC_2R)$ homologues, **1** (where R = C_6H_5) and **2** (where R = C_6F_5), which primarily differ from each other by a coordination of the carbonyl ligand to two Rh atoms in one complex and to all three Rh atoms in the other complex.

Stereochemical Relationship of the $[Fe_3(CO)_9(\mu\text{-}CO)(\mu_3\text{-}CO)]^{2-}$ Dianion with $Fe_3(CO)_{10}(\mu\text{-}CO)_2$, the $[Fe_3(CO)_{10}(\mu\text{-}H)(\mu\text{-}CO)]^-$ Monoanion, and $Fe_3(CO)_{10}(\mu\text{-}H)(\mu\text{-}COMe)$, and Resulting Bonding Implications. (a) General Remarks. A comparison of the geometry of the $[Fe_3(CO)_{11}]^{2-}$ dianion with those of the $Fe_3(CO)_{12}$ molecule (which may be formulated as $Fe_3(CO)_{10}(\mu\text{-}CO)_2$) and the $[HFe_3(CO)_{11}]^-$ monoanion (which may likewise be formulated as $[Fe_3(CO)_{10}(\mu\text{-}H)(\mu\text{-}CO)]^-$) as well as with that of the O-methylated species $Fe_3(CO)_{10}(\mu\text{-}H)(\mu\text{-}COMe)$[34-36] of the monoanion is particularly informative. First, it should be realized that the geometry of the $[Fe_3(CO)_9(\mu\text{-}CO)(\mu_3\text{-}CO)]^{2-}$ dianion (displayed in Figure 2) may be conceptually constructed in either of two ways from that of $Fe_3(CO)_{10}(\mu\text{-}CO)_2$ upon the replacement of one carbonyl ligand with an electron pair. One way involves the abstraction of one of the two doubly bridging carbonyl ligands with a concomitant tipping of the *cis*-$Fe(CO)_4$ group in order to transform a terminal axial carbonyl into a triply bridging carbonyl, which thereby fills the missing combination site about each of the two equivalent iron atoms. The second way conversely involves the abstraction of one of the two axial carbonyls of the *cis*-$Fe(CO)_4$ group with the concomitant movement of one doubly bridging

(27) Delbaere, L. T. J.; Kruczynski, L. J.; McBride, D. W. *J. Chem. Soc., Dalton Trans.* **1973**, 307–10.

(28) Barnett, B. L.; Krüger, C. *Angew Chem., Int. Ed. Engl.* **1971**, *10*, 910–1.

(29) With the presence of two additional valence electrons, an $Fe_3(CO)_9(\mu_3\text{-}X)(\mu_3\text{-}Y)$ complex possesses a different basic type geometry containing an isosceles iron triangle with one nonbonding side and two electron-pair bonding sides, as illustrated by the structurally determined molecules of $Fe_3(CO)_9(\mu_3\text{-}X)_2$ (where X = S,[30a] Se,[30b] Te,[30c] NR,[30d] and PR[30e]). Each of these latter electronically equivalent systems is presumed by a localized metal cluster model[31] to have these extra two electrons occupy an in-plane antibonding metal cluster MO such that their removal by formation of a hypothetical dication, which would be electronically equivalent to the $Fe_3(CO)_9(\mu_3\text{-}As)_2$ molecule (or to the $[Fe_3(CO)_9(\mu\text{-}CO)(\mu_3\text{-}CO)]^{2-}$ dianion), should likewise produce a completely bonding iron triangle.

(30) (a) Wei, C. H.; Dahl, L. F. *Inorg. Chem.* **1965**, *4*, 493–9; Huntsman, J. R. Ph.D. Thesis, University of Wisconsin—Madison, 1973. (b) Dahl, L. F.; Sutton, P. W. *Inorg. Chem.* **1963**, *2*, 1067–9. (c) Nelson, L. L.; Dahl, L. F., submitted for publication. (d) Baikie, P. E.; Mills, O. S. *Chem. Commun.* **1967**, 1228–9. Doedens, R. J. *Inorg. Chem.* **1969**, *8*, 570–4. (e) Huntsman, J. R. Ph.D. Thesis, University of Wisconsin—Madison, 1973.

(31) (a) Strouse, C. E.; Dahl, L. F. *Discuss. Faraday Soc.* **1969**, *47*, 93–106. Strouse, C. E.; Dahl, L. F. *J. Am. Chem. Soc.* **1971**, *93*, 6032–41. Teo, B. K., Ph.D. Thesis, University of Wisconsin—Madison, 1973.

(32) The different bridging carbonyl arrangement determined for these two diamagnetic homologues was rationalized on the basis of electronic effects involving the nature of the acetylene substituents. The molecular configurations of both compounds **1** and **2** similarly consist of a completely bonding triangular array of $Rh(\eta^5\text{-}C_5H_5)$ fragments linked not only by electron-pair Rh–Rh bonds but also by the olefinic-shaped acetylene ligand with a μ-type bond coordination with two Rh_B atoms and a σ-type bond coordination to the third Rh_A atom. The fact that in **1** the carbonyl is a triply bridging ligand on the opposite side of the trirhodium plane from the diphenylacetylene ligand in contrast to it in **2** being a doubly bridging ligand to both Rh_B atoms on the same side of the trirhodium plane as the bis(pentafluorophenyl)acetylene is attributed from orbital energy arguments to the relatively better π-donor and poorer π^* back-bonding interaction of the $C_6H_5C_2C_6H_5$ ligand with Rh_A in comparison with that of the $C_6F_5C_2C_6F_5$ ligand which thereby allows the carbonyl ligand to compete effectively in **1** as a π acceptor from the Rh_A. In the case of the $C_6F_5C_2C_6F_5$ ligand the charge is sufficiently delocalized from the Rh_A to the lower energy π^*(olefin) orbital to render unstable the Rh_A–CO bond in favor of the observed geometry in **2**.

(33) Trinh-Toan; Broach, R. W.; Gardner, S. A.; Rausch, M. D.; Dahl, L. F. *Inorg. Chem.* **1977**, *16*, 279–89.

(34) Shriver, D. F.; Lehman, D.; Strope, D. *J. Am. Chem. Soc.* **1975**, *97*, 1594–6.

(35) It is noteworthy that $H_2Fe_3(CO)_{11}$, which may now be formulated as the O-protonated analogue, $Fe_3(CO)_{10}(\mu\text{-}H)(\mu\text{-}COH)$, was recently shown unequivocally from temperature-dependent ^1H and ^{13}C NMR studies by Shriver and co-workers[36] to be the first example of a metal carbonyl hydride in which a proton is bonded to the oxygen of a carbonyl ligand.

(36) Hodali, H. A.; Shriver, D. F.; Ammlung, C. A. *J. Am. Chem. Soc.* **1978**, *100*, 5239–40.

Table IV. Comparison of Mean Geometrical Parameters for the $[Fe_3(CO)_{11}]^{2-}$ Dianion with Those for Other Triangularly Bonded Triiron Carbonyl Clusters Containing Twelve Ligands

species	$[Fe_3(CO)_{11}]^{2-}$ [a]	$[HFe_3(CO)_{11}]^-$ [b]	$HFe_3(CO)_{10}(COMe)$ [c]	$Fe_3(CO)_{12}$ [d]
structural formulation	$[Fe_3(CO)_9(\mu\text{-}CO)(\mu_3\text{-}CO)]^{2-}$	$[Fe_3(CO)_{10}(\mu\text{-}H)(\mu\text{-}CO)]^-$	$Fe_3(CO)_{10}(\mu\text{-}H)(\mu_2\text{-}COMe)$	$Fe_3(CO)_{10}(\mu\text{-}CO)_2$
crystallographic site symmetry	C_s-m	C_1-1	C_1-1	C_i-$\bar{1}$ [e]
virtual symmetry	C_s-m	C_s-m	C_s-m [f]	C_2-2 [g]
		A. Distances (Å)		
Fe_A–Fe_B [h]	[2][i] 2.593 (2)	[2] 2.690 (3)	[2] 2.667 (2)[j]	[2] 2.680 (2)[j]
Fe_B–$Fe_{B'}$	[1] 2.603 (3)	[1] 2.577 (3)	[1] 2.596 (2)	[1] 2.558 (1)
Fe_B–CO(DB)[k]	[2] 1.96 (1)	[2] 1.92 (1)[j]	[2] 1.85 (1)[j]	[2] 1.95 (4), 2.16 (4)[j]
$Fe_A\cdots$CO(DB)	[1] 2.72 (1)	[1] 3.00 (1)	[1] 2.70 (1)	[2] 3.28 (4)[j]
C(DB)–O(DB)	[1] 1.18 (1)	[1] 1.20 (1)	[1] 1.30 (1)	[2] 1.13 (5)[j]
$Fe_B\cdots C_{Ax(d)}$ [l]		[1][m] 2.96 (1), 3.06 (1)	[1][m] 2.85 (1), 2.95 (1)	[1][m] 3.07 (4), 3.19 (4)
$Fe_B\cdots C_{Ax(u)}$	[2] 3.51 (1)	[1] 3.11 (1), 3.21 (1)	[1] 3.26 (1), 3.24 (1)	[1] 3.19 (4), 3.24 (4)
Fe_B–CO(TB)[k]	[2] 2.21 (1)			
Fe_A–CO(TB)	[1] 1.85 (1)			
C(TB)–O(TB)	[1] 1.21 (1)			
		B. Bond Angles (Deg)		
Fe_B–C(DB)–$Fe_{B'}$	[1] 83.1 (6)	[1] 84.4 (5)	[1] 89.3 (4)	[2] 77 (3)
Fe_A–C(TB)–Fe_B	[2] 78.8 (4)			
Fe_B–C(TB)–$Fe_{B'}$	[1] 72.1 (4)			
		C. Torsional Angles (Deg)[m]		
Fe_3–$Fe_BFe_{B'}$C(DB) fragment	92	102	91	112
Fe_3–$Fe_BFe_{B'}$C(TB) fragment	53			

[a] This work. [b] Reference 3. [c] Reference 34. [d] Reference 2b. [e] The crystal structure is disordered with each molecule randomly distributed in two orientations which are related to each other by a crystallographic center of symmetry. [f] The oxygen-linked methyl substituent, displaced to one side of the pseudomirror plane, lowers the molecular symmetry to C_1-1. [g] Due to the two chemically equivalent bridging carbonyl ligands each being distinctly asymmetrical with one short and one long Fe–C bond length. [h] Fe_A denotes the unique apical iron atom, while Fe_B designates the other two equivalent basal iron atoms. [i] Brackets enclose the number of equivalent distances having the values listed in the right columns. [j] Each esd given in parentheses after the mean of equivalent observations represents the estimated standard deviation of an individual observation rather than that of the mean. [k] CO(DB) and CO(TB) denote a doubly and triply bridged carbonyl ligand, respectively. [l] $C_{Ax(d)}$ and $C_{Ax(u)}$ designate the axial carbonyl carbon atoms located on the opposite (down) and same (up) triiron face, respectively, as the C(DB)–O(DB) ligand. [m] Both values are given under C_1 symmetry rather than the mean under pseudo-C_s symmetry. [n] The torsional angle of the designated fragment denotes the angle between the triiron plane and the plane defined by the two Fe_B atoms and either the C(DB) or C(TB) atom.

carbonyl to give a resulting triply bridging carbonyl. Similarly, the $[Fe_3(CO)_9(\mu\text{-}CO)(\mu_3\text{-}CO)]^{2-}$ dianion may be formally derived by deprotonation of the $[Fe_3(CO)_{10}(\mu\text{-}H)(\mu\text{-}CO)]^-$ monoanion followed by a tipping of the *cis*-$Fe(CO)_4$ group to transform an axial carbonyl into a triply bridging carbonyl.

These constructs stress that to a first approximation the three terminal carbonyl ligands on each of the equivalent Fe(2) and Fe(2′) atoms (designated for comparative analysis as Fe_B) as well as the two equatorial ligands on the unique Fe(1) (also denoted hereafter as Fe_A) are not intimately connected with a formal interconversion of their static geometries (i.e., ligand exchange or carbonyl scrambling effects are ignored here). For analysis of the different modes of carbonyl bridging for these four triangular iron clusters, selected distances, bond angles, and torsional angles are presented in Table IV.

(b) Electron-Pair Fe–Fe Bonds. An examination in Table IV of the one Fe_B–$Fe_{B'}$ distance and two equivalent Fe_A–Fe_B distances for each of the four triiron carbonyl clusters reveals only the iron triangle in the $[Fe_3(CO)_9(\mu\text{-}CO)(\mu_3\text{-}CO)]^{2-}$ dianion is essentially equilateral as opposed to the isosceles triangles of iron atoms in the other three compounds. It is further observed that the two Fe_A–Fe_B bonds are longer but that the one Fe_B–$Fe_{B'}$ bond is shorter in the $[Fe_3(CO)_{10}(\mu\text{-}H)(\mu\text{-}CO)]^-$ monoanion (2.690 (3), 2.577 (3) Å), in $Fe_3(CO)_{10}(\mu\text{-}H)(\mu\text{-}COMe)$ (2.667 (2), 2.596 (2) Å), and in $Fe_3(CO)_{10}(\mu\text{-}CO)_2$ (2.680 (2), 2.558 (1) Å) than the corresponding ones in the $[Fe_3(CO)_9(\mu\text{-}CO)(\mu_3\text{-}CO)]^{2-}$ dianion (2.593 (2), 2.603 (3) Å). The degree of distortion of the equilateral iron triangle into an isosceles one is ascribed mainly to the particular carbonyl-bridged arrangement (coupled with the negative charge) and is not presumed to reflect any differences in individual Fe–Fe bond orders, which from qualitative electronic considerations are each assumed to be 1.0.

(c) Analysis of the Doubly Bridging Carbonyl Ligand CO(DB) with Respect to Evidence for Semibridging to the Third Iron Atom Fe_A in the $[Fe_3(CO)_9(\mu\text{-}CO)(\mu_3\text{-}CO)]^{2-}$ Dianion. Whereas the $[Fe_3(CO)_9(\mu\text{-}CO)(\mu_3\text{-}CO)]^{2-}$ and $[Fe_3(CO)_{10}(\mu\text{-}H)(\mu\text{-}CO)]^-$ anions both possess a symmetrical doubly bridging carbonyl ligand

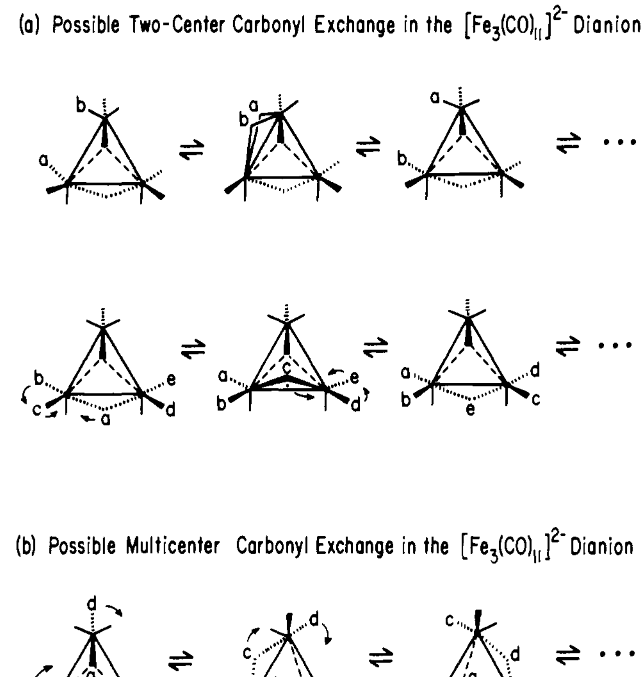

Figure 4. Schematic diagram showing two possible mechanisms of carbonyl exchange in the $[Fe_3(CO)_{11}]^{2-}$ dianion. Neither of these mechanisms allows for the exchange of the unique triply bridging carbonyl ligand with the other carbonyl ligands.

due to crystallographic and chemical mirror plane symmetry, respectively, the $Fe_3(CO)_{10}(\mu\text{-}CO)_2$ molecule conforms to C_2-2 rather than C_{2v}-$2mm$ symmetry due to the existence of two unsymmetrical bridging carbonyl ligands linking the two equivalent

Fe_B and $Fe_{B'}$ atoms in a compensatory fashion.[37-42] Table IV shows that the Fe_B–CO(DB) and C(DB)–O(DB) bond lengths of 1.96 (1) and 1.18 (1) Å, respectively, in the dianion compare favorably with the corresponding values of 1.92 (1) and 1.21 (1) Å, respectively, in the monoanion. These values are expectedly different from those in the neutral O-methylated derivative of the monoanion $Fe_3(CO)_{10}(\mu\text{-H})(\mu\text{-COMe})$ for which the average Fe_B–CO(DB) distance is 0.07 Å smaller and the C(DB)–O(DB) distance is 0.10 Å larger than those in the monoanion.

Of prime interest is that the distance of 2.72 (1) Å between the bridging carbonyl C(DB) atom and the third iron atom Fe_A in the dianion is virtually identical with the corresponding value of 2.70 (1) Å previously found by Shriver and co-workers[34] for the structure of $Fe_3(CO)_{10}(\mu\text{-H})(\mu\text{-COMe})$. This similar disposition of the CO(DB) ligand relative to the iron triangle in these two complexes is also reflected in the torsional angle between the triiron plane and the plane defined by C(DB) and both Fe_B atoms being 92° in the dianion vs. 91° in the $Fe_3(CO)_{10}(\mu\text{-H})(\mu\text{-COMe})$ molecule. On the basis that the above values for the latter O-methylated molecule are considerably smaller than the corresponding values of 3.00 (1) Å and 102°, respectively, found in the parent monoanion, Shriver et al.[34] proposed that this marked structural alteration is associated with an electron-acceptor induced shift of the CO(DB) ligand due to O-methylation from a double-metal bridge to a triple-metal bridge. They also suggested that symmetry in the bonding is achieved by a concomitant shift of the axial carbonyl ligand (coordinated to Fe_A) on the opposite face of the triangle toward the Fe_B and $Fe_{B'}$ atoms. They pointed out that the general rule consistent with these observations is "that the attachment of an electron acceptor to a carbonyl oxygen increases the propensity for bridge formation at the carbon end".

Although these acceptor–donor arguments no doubt are valid in general, the unusually long Fe_A–C(DB) distances of 2.70 (1) Å in $Fe_3(CO)_{10}(\mu\text{-H})(\mu\text{-COMe})$ and 2.72 (1) Å in the dianion are typical values for closest intramolecular nonbonding Fe···CO distances in other compounds,[43] and hence they would appear to support at most only a very weak bonding interaction. In this connection, compounds containing the most highly unsymmetrical (but still detectable) doubly bridging carbonyl ligands include (1) $Fe_3(CO)_8(SC_4H_8)_2$,[39] in which there are two twofold-related borderline-bridging carbonyl ligands with Fe–CO distances of 1.76 (1) and 2.55 (1) Å with a Fe–C–O bond angle of 167.4 (7)°, (2) $Fe_2(CO)_6(C_4Me_2(OH)_2)$,[44] in which a carbonyl ligand (of 1.74 Å bond length from one iron atom and with a Fe–C–O bond angle of 168°) has a second Fe–CO distance of 2.48 Å, (3) $Fe_2(CO)_6$(1,7-cyclodecadiyne),[45] in which a bridging carbonyl has Fe–CO distances of 1.75 (2) and 2.32 (2) Å and a Fe–C–O bond angle of 162 (3)°, and (4) $Fe_2(CO)_7$(bipy),[42] in which a bridging carbonyl possesses Fe–CO distances of 1.80 and 2.37 Å and a Fe–C–O bond angle of 160.5°. On the basis of these examples, it is our view that any bonding interaction between the CO(DB) ligand and Fe_A in the $[Fe_3(CO)_9(\mu\text{-CO})(\mu_3\text{-CO})]^{2-}$ dianion as well as in $Fe_3(CO)_{10}(\mu\text{-H})(\mu\text{-COMe})$ is minimal. Nevertheless, an indication of the occurrence of a slight analogous interaction of the C(DB) atom with Fe_A in the dianion is given by the O(DB) atom (i.e., labeled O(1)) being displaced from the Fe_BC(DB)$Fe_{B'}$ plane (Table III, 4) by 0.07 Å away from Fe_A; this small deviation of O(DB) from coplanarity expected for a doubly bridging carbonyl is directionally consistent with the C(DB) atom being pulled slightly toward Fe_A due to a small bonding interaction. In the case of the O-methylated molecule which has two axial and two equatorial carbonyl ligands attached to Fe_A, it is presumed that intramolecular steric effects may effectively prevent a closer approach of the doubly bridged COMe ligand to Fe_A.

(d) The Unsymmetrically Bound, Triply Bridging Ligand CO(TB). The triply bridging carbonyl ligand in the $[Fe_3(CO)_9(\mu\text{-CO})(\mu_3\text{-CO})]^{2-}$ dianion is 0.36 Å nearer to the Fe_A atom Fe(1) than to the two Fe_B atoms Fe(2) and Fe(2′). This particular asymmetrical bridging character is not at all surprising in view of the stereochemically different environment of Fe_A from that of the two Fe_B atoms due to the doubly bridging carbonyl ligand being exclusively coordinated to the latter two iron atoms. A shorter Fe_A–CO(triply bridging) bond would be expected from orbital energetic arguments in order to provide (at least) a partial equalization of the competitive π-acceptor interactions of the two bridging carbonyl ligands with the three bonded $Fe(CO)_3$ fragments (vide supra).

Although no triply bridging carbonyl ligand is found in the other known triiron carbonyl and carbonyl hydride clusters presented herein, structural studies have revealed the existence of such a ligand in other iron carbonyl clusters including the $[Fe_4(CO)_{13}]^{2-}$ dianion,[43] $Fe_3(CO)_9(\mu_3\text{-CO})(\mu_3\text{-NSiMe}_3)$,[28] and $[Fe_4(\eta^5\text{-}C_5H_5)_4(\mu_3\text{-CO})_4]^n$ (n = 0,[46a] 1+[46b]). In fact, the pseudo C_3 geometry of the $[Fe_4(CO)_{13}]^{2-}$ dianion, which has three carbonyls in the basal triiron plane adopting a highly asymmetrical doubly bridging configuration, was initially considered by us (prior to the research reported here) to be geometrically related to the structural model (consisting of two symmetrically linked, triply bridging carbonyls), initially proposed[15] for the $[Fe_3(CO)_{11}]^{2-}$ dianion, by the formal replacement of one of the two triply bridging, two-electron-donating carbonyl ligands with a triply bridging, two-electron-donating $Fe(CO)_3$ fragment. Both the one 1.85 (1) and two 2.21 (1) Å distances (mean 2.09 Å) from the C(TB) atom to the three iron atoms in the $[Fe_3(CO)_{11}]^{2-}$ dianion as well as the C(TB)–O(TB) bond length of 1.21 (1) Å may be compared with the corresponding average values for the equidistant, triply bridging carbonyls in the $[Fe_4(CO)_{13}]^{2-}$ dianion (2.00, 1.20 (3) Å),[43] in $Fe_3(CO)_9(\mu_3\text{-CO})(\mu_3\text{-NSiMe}_3)$ (2.06 (1), 1.17 (1) Å),[28] and in the neutral $Fe_4(\eta^5\text{-}C_5H_5)_4(\mu_3\text{-CO})_4$ molecule (1.99, 1.20 Å).[46a]

(37) The existence of unsymmetrical carbonyl bridges in $Fe_3(CO)_{10}(\mu\text{-CO})_2$ was first proposed from an X-ray investigation by Dahm and Jacobson[38] of the crystal structure of $Fe_3(CO)_9(PPh_3)(\mu\text{-CO})_2$, which exists in the solid state as a 1:1 mixture of two geometrical isomers: one (isomer A) with the triphenylphosphine ligand substituted in place of the terminal equatorial carbonyl group on one of the bridging carbonyl iron atoms and the other (isomer B) with the triphenylphosphine ligand coordinated to the nonbridged iron atom at one of the two equatorial sites. Since the molecular configuration of both isomers showed each of the two bridging carbonyls to be unsymmetrically coordinated to the iron atoms with shorter Fe–CO(bridging) distances of average value 1.87 (2) Å vs. longer Fe–CO(bridging) distances of average value 2.04 (2) Å, Dahm and Jacobson[38] concluded that this bridging carbonyl asymmetry is more likely a property of the unsubstituted parent compound rather than an effect produced by the triphenylphosphine ligand. Despite the large variations in the individual distances and bond angles in the averaged disordered structure of $Fe_3(CO)_{10}(\mu\text{-CO})_2$, Wei and Dahl[2a] concluded from the anisotropic least-squares refinement (film data) that the two bridging carbonyl groups are indeed somewhat unsymmetrical, so that the $Fe_3(CO)_{10}(\mu\text{-CO})_2$ molecule can be considered within a good approximation to possess C_2 symmetry rather than C_{2v} symmetry.

A greatly improved resolution of the molecular structure, provided by the application of modern diffractometry techniques, enabled Cotton and Troup[2b] to establish clearly the C_2 molecular geometry in showing that the two bridging carbonyl ligands are distinctly unsymmetrical with mean short and long Fe–C bond lengths of 1.94 and 2.16 Å, respectively, for which the individual esd's are 0.02–0.04 Å. Cotton and Troup[39] subsequently prepared and structurally characterized a related triangular iron complex triiron octacarbonylbis(tetrahydrothiophene), which together with $Fe_3(CO)_7(PMe_2Ph)_3(\mu\text{-CO})_2$[40] provided a basis for their analysis[39,41] of the varying extent of compensatory asymmetry found for the two bridging carbonyls in the $Fe_3L_{10}(\mu\text{-CO})_2$ type of molecule. Cotton and Troup[38,41,42] suggested a classification of asymmetrical carbonyl bridges into two broad categories: (1) those occurring in compensatory or conjugate pairs, as exemplified above, with the direction of asymmetry of one member of the pair opposite to that of the other such that the metal atoms are symmetry equivalent; (2) those occurring in noncompensatory fashion with nonequivalence of metal atoms. They also advocated that unsymmetrical carbonyl bridges of class 1 observed in the solid state merely represent "stopped-action" views of the intermediate stages of concerted opening and closing of pairs of carbonyl bridges in metal carbonyl clusters which undergo fast carbonyl scrambling and isomerization processes in solution.

(38) Dahm, D. J.; Jacobson, R. A. *J. Am. Chem. Soc.* **1968**, *90*, 5106–12.
(39) Cotton, F. A.; Troup, J. M. *J. Am. Chem. Soc.* **1974**, *96*, 5070–3.
(40) Raper, G.; McDonald, W. S. *J. Chem. Soc. A* **1971**, 3430–2.
(41) Cotton, F. A. *Prog. Inorg. Chem.* **1974**, *21*, 1–28.
(42) Cotton, F. A.; Troup, J. M. *J. Am. Chem. Soc.* **1974**, *96*, 1233–4.
(43) Doedens, R. J.; Dahl, L. F. *J. Am. Chem. Soc.* **1966**, *88*, 4847–55.
(44) Hoch, A. A.; Mills, O. S. *Acta Crystallogr.* **1961**, *14*, 139–148.
(45) Chin, H. B.; Bau, R. *J. Am. Chem. Soc.* **1973**, *95*, 5068–70.
(46) (a) Neuman, M. A.; Trinh-Toan; Dahl, L. F. *J. Am. Chem. Soc.* **1972**, *94*, 3383–8. (b) Trinh-Toan; Fehlhammer, W. P.; Dahl, L. F. *Ibid.* **1972**, *94*, 3389–97.

Analysis of the Spectral Data for the $[Fe_3(CO)_9(\mu\text{-}CO)(\mu_3\text{-}CO)]^{2-}$ Dianion in Terms of Its Solid-State Geometry. (a) Mössbauer Data. The insensitivity of a room-temperature Mössbauer spectrum, which for $[Fe(en)_3]^{2+}[Fe_3(CO)_{11}]^{2-}$ was reported[10] to show an unbroadened quadrupole-split doublet for the dianion, to differentiate between the different environments of the two kinds of iron atoms is not surprising. Attempts by Mössbauer spectroscopy[10,47a] on other polynuclear iron clusters (e.g., $[NEt_4]_2{}^+[Fe_4(CO)_{13}]^{2-}$, $Fe_4(NO)_4(\mu_3\text{-}S)_2(\mu_3\text{-}NCMe_3)_2$,[48] and the Roussin black $[Fe_4(NO)_7(\mu_3\text{-}S)_3]^-$ monoanion[49]) to observe unequivocally via a four-line Mössbauer spectrum the two crystallographically different types of iron atoms in each complex have also been unsuccessful. A room-temperature Mössbauer spectrum[10] of $[NEt_4]_2{}^+[Fe_4(CO)_{13}]^{2-}$ exhibited only a poorly resolved quadrupole doublet and hence did not distinguish between the dissimilar environments of the one apical iron and three basal iron atoms. Likewise, a recent comprehensive study by Sedney and Reiff[47a] of the high-resolution, zero-field Mössbauer spectra (over a temperature range 1.6–300 K) of the cubane-like $Fe_4(NO)_4(\mu_3\text{-}S)_2(\mu_3\text{-}NCMe_3)_2$ molecule and of the ammonium salt of the Roussin black anion gave from a least-squares analysis of the spectral data for each of these compounds only a single quadrupole doublet. This work[47a] is in contradistinction to a previous temperature-dependent Mössbauer investigation[47b] which for the ammonium Roussinate salt indicated the existence of two overlapping quadrupole doublets arising from the apical and basal iron atoms being in the crystallographically known 1:3 ratio.[50] Greenwood and co-workers,[10] in citing the failure of the Mössbauer technique to distinguish between the structurally different iron environments in the $[Fe_4(CO)_{13}]^{2-}$ dianion, cautioned that care must be exercised in arriving at interpretations based upon quadrupole splittings because similar electric field gradients can be produced by different environments. This same problem was discussed by Sedney and Reiff.[47a]

(b) Infrared Data. The solid-state configuration for the $[Fe_3(CO)_9(\mu\text{-}CO)(\mu_3\text{-}CO)]^{2-}$ dianion would appear to be not incompatible (as yet) with its infrared solution spectra in the carbonyl stretching region, provided that one ignores the occurrence of fewer unresolved terminal carbonyl bands than those expected from group theoretical predictions (which often is the case in the room-temperature IR spectra of other polynuclear metal carbonyls). The observed carbonyl spectral pattern obtained from a THF solution of the tetraethylammonium salt exhibits absorption maxima at 1938 (s), 1910 (ms), and 1890 (sh) cm^{-1}, which are attributed to the terminal carbonyls along with a broad band at 1670 (w) cm^{-1} which is ascribed to the doubly bridging carbonyl. This latter assignment is based upon the nearness of this 1670-cm^{-1} band to the low-frequency carbonyl band of 1735 (m) cm^{-1} (which from negative charge considerations is expectedly higher) reported by Wilkinson and Todd[51] for $[NEt_4]^+[Fe_3(CO)_9(\mu\text{-}H)(\mu\text{-}CO)]^-$ in acetonitrile solution. A weak absorption band for the triply bridging carbonyl ligand would be expected in the 1550–1600-cm^{-1} region (which is obscured by absorption bands of polar solvents such as THF and DMF). It is pertinent that the 1595-cm^{-1} band found by Greenwood and co-workers[10] in a Nujol mull spectrum of $[Fe(en)_3]^{2+}[Fe_3(CO)_{11}]^{2-}$ was tentatively assigned by them to triply bridging carbonyl ligands.

Of relevance is the fact that the infrared solution spectra[52,53] of $Fe_3(CO)_{12}$ are very different in the carbonyl stretching region both from polarized single-crystal IR spectra[54] of $Fe_3(CO)_{12}$ and from an argon-matrix IR spectrum[55] at 20 K in *not* being reconcilable with its solid-state molecular configuration. A detailed examination of the highly fluxional character of triiron dodecacarbonyl in solution led Cotton and Hunter[53] to propose that its IR solution spectra as well as ^{13}C NMR spectra (vide infra) can be attributed to a continuous range of structures with varying degrees of asymmetry of the two doubly bridging carbonyls from a nonbridged D_{3h} $Os_3(CO)_{12}$-type configuration to a C_{2v} configuration with symmetrical bridges. An alternative explanation was put forth by Johnson,[56] who, on the basis of the assumption that the icosahedral carbonyl arrangement about the triiron core is maintained during the fluxional process and that equilibration of these ligands is brought about by the orientation of the iron triangle within the carbonyl icosahedron, suggested the possible existence of a new isomeric form of $Fe_3(CO)_{12}$ in solution.

Hence, the distinct possibility that the bridging carbonyls of the $[Fe_3(CO)_{11}]^{2-}$ dianion may likewise adopt varying degrees of asymmetry or perhaps even different bonding modes in solution should not be overlooked, but a further detailed experimental study is needed in order to test this possibility.

(c) ^{13}C NMR Data. A preliminary ^{13}C NMR study of the $[Fe_3(CO)_{11}]^{2-}$ dianion by Heaton,[18] who found only a sharp singlet even at low temperatures, indicates a small barrier to complete equilibration in solution of the seven different carbonyl environments of the solid-state configuration. In this connection, it is informative to examine briefly the observations and interpretations of the dynamic behavior in solution of the closely related $Fe_3(CO)_{12}$ molecule and of the corresponding $[HFe_3(CO)_{11}]^-$ monoanion and its O-methylated neutral derivative in order to provide insight concerning the nature of the ligand migration processes proposed here for the $[Fe_3(CO)_{11}]^{2-}$ dianion in solution. A comprehensive review of the mechanistic features of metal cluster rearrangements including those of $Fe_3(CO)_{12}$ and of the $[HFe_3(CO)_{11}]^-$ monoanion has been recently presented by Band and Muetterties.[59]

Room-temperature ^{13}C NMR spectra of $Fe_3(CO)_{12}$ likewise show a sharp singlet[53,57,58] which persists down to 123 K[53] thereby verifying the prediction of Cotton and Troup[2b] that the activation energy for the complete carbonyl scrambling in solution is ≤ 5 kcal mol^{-1}. Exchange mechanisms proposed for a facile migration of carbonyl ligands include the pairwise bridge–terminal interchange model (in which in this case the $Fe_3(CO)_{12}$ molecules exhibit in solution a full range of two unsymmetrical bridging carbonyls varying in limit from an idealized symmetrical bridging C_{2v} configuration to a nonbridged D_{3h} configuration) advocated by Cotton and co-workers[2b,41,53] and the concerted motion of all carbonyl ligands relative to the triiron core (vide supra) proposed by Johnson.[56] This latter model, which has been extended[60–62] to other metal carbonyl clusters, has been criticized by others.[63,64]

^{13}C NMR spectra for the $[HFe_3(CO)_{11}]^-$ monoanion show only one carbonyl peak at room temperature but two signals at −30 °C.[51,58] A limiting spectrum consistent with the solid-state configuration appears to be reached at −107 °C with seven peaks in a 1:1:1:2:2:2:2 intensity ratio.[51] In order to account for the observed data, Wilkinson and Todd[51] proposed that in the low-

(47) (a) Sedney, D.; Reiff, W. M. *Inorg. Chim. Acta* **1979**, *34*, 231–6. (b) Kostiner, E.; Steger, J.; Rea, J. R. *Inorg. Chem.* **1970**, *9*, 1939–41. (c) Kerler, W.; Neuwirth, W.; Fluck, E.; Kuhn, P.; Zimmerman, B. *Z. Phys.* **1963**, *173*, 321–356.
(48) Gall, R. S.; Chu, C. T.-W.; Dahl, L. F. *J. Am. Chem. Soc.* **1974**, *96*, 4019–23.
(49) (a) Johansson, G.; Lipscomb, W. N. *Acta Crystallogr.* **1958**, *11*, 594–8; *J. Chem. Phys.* **1957**, *27*, 1417. (b) Chu, C. T.-W.; Dahl, L. F. *Inorg. Chem.* **1977**, *16*, 3245–51.
(50) An initial room-temperature Mössbauer spectrum[47c] of the hydrated sodium salt of the Roussin black monoanion indicated only a single type of iron environment.
(51) Wilkinson, J. R.; Todd, L. J. *J. Organomet. Chem.* **1976**, *118*, 199–204.
(52) Knight, J.; Mays, M. *Chem. Commun.* **1970**, 1006–7.
(53) Cotton, F. A.; Hunter, D. L. *Inorg. Chim. Acta* **1974**, *11*, L9–10.
(54) Dahl, L. F.; Rundle, R. E. *J. Chem. Phys.* **1957**, *27*, 323–4.
(55) Poliakoff, M.; Turner, J. J. *Chem. Commun.* **1970**, 1008–9.
(56) Johnson, B. F. G. *J. Chem. Soc., Chem. Commun.* **1976**, 703–4.
(57) Gansow, O. A.; Burke, A. R.; Vernon, W. D. *J. Am. Chem. Soc.* **1972**, *94*, 2550–2.
(58) Forster, A.; Johnson, B. F. G.; Lewis, J.; Matheson, T. W.; Robinson, B. H.; Jackson, W. G. *J. Chem. Soc., Chem. Commun.* **1974**, 1042–4.
(59) Band, E.; Muetterties, E. L. *Chem. Rev.* **1978**, *78*, 639–58.
(60) Evans, J.; Johnson, B. F. G.; Lewis, J.; Matheson, T. W.; Norton, J. R. *J. Chem. Soc., Dalton Trans.* **1978**, 626–34.
(61) Johnson, B. F. G.; Benfield, R. E. *J. Chem. Soc., Dalton Trans.* **1978**, 1554–68.
(62) Evans, J. *Adv. Organomet. Chem.* **1977**, *16*, 319–47.
(63) Cotton, F. A.; Hanson, B. E.; Jamerson, J. D. *J. Am. Chem. Soc.* **1977**, *99*, 6588–94.
(64) Hitchcock, P. B.; Mason, R.; Textor, M. *J. Chem. Soc., Chem. Commun.* **1976**, 1047–8.

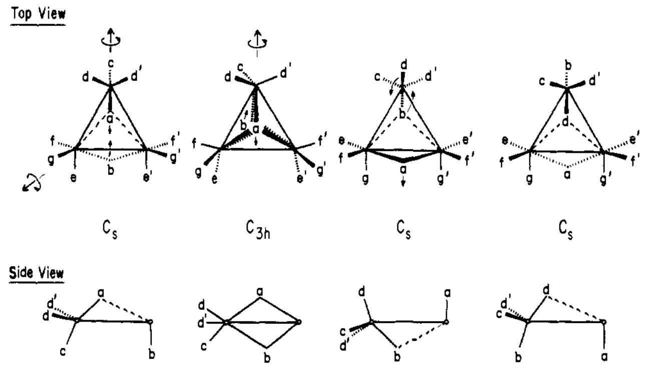

Figure 5. Schematic diagram showing for the $[Fe_3(CO)_{11}]^{2-}$ dianion a proposed terminal-face-edge carbonyl-exchange model. This proposed new kind of possible mechanistic pathway involves a synchronous motion of a terminal axial carbonyl on the unique Fe_A atom and both bridging carbonyls over both triangular faces. This model thereby allows an exchange of the triply bridging carbonyl with the other carbonyl ligands.

temperature process the environments of the one doubly bridging carbonyl and one of the axial carbonyl ligands on the third iron atom, Fe_A, are selectively averaged by a pairwise opening and closing of the bridging hydrogen and bridging carbonyl, while the environments of the other nine terminal carbonyls are separately averaged. This particular carbonyl scrambling was deemed[59] to be consistent with a multicenter ligand exchange. Wilkinson and Todd[51] also pointed out that their IR and ^{13}C NMR studies of the $[HFe_3(CO)_{11}]^-$ monoanion in various solution environments show the basic character of the bridging carbonyl in the monoanion which forms base-acid complexes with BF_3 as well as with the $[HNEt_3]^+$ cation. They suggested that these base-acid interactions cause the fluxional processes of the $[HFe_3(CO)_{11}]^-$ monoanion to stop at a higher temperature. The methylation[34] and protonation[36] of the bridging carbonyl in the $[HFe_3(CO)_{11}]^-$ monoanion to give $HFe_3(CO)_{10}(COMe)$ and $HFe_3(CO)_{10}(COH)$, respectively, was conclusively shown by Shriver and co-workers[36] to occur in solution from comparative low-temperature ^{13}C NMR spectra (−100 °C) with that of the monoanion (as the PPN^+ salt at −120 °C) on the basis of the similarities of their chemical shifts and splitting patterns demonstrating analogous limiting structures in solution.

The fact that the $[Fe_3(CO)_{11}]^{2-}$ dianion may be regarded as a "defect" structure[59] of $Fe_3(CO)_{12}$ in the same fashion as the $[Rh_6(CO)_{15}]^{2-}$ dianion (which is fluxional at −70 °C[65]) is considered to be a defect analogue of $Rh_6(CO)_{16}$[66] (which is rigid at +70 °C[65]) suggests in accordance with the defect argument by Band and Muetterties[59] that the $[Fe_3(CO)_{11}]^{2-}$ dianion likewise possesses an even lower barrier to carbonyl ligand migration than that of only ≤5 kcal mol^{-1} estimated[2b,53] for $Fe_3(CO)_{12}$. However, neither a simple pairwise- nor a multicenter-exchange mechanism (Figure 4) appears to be sufficient to rationalize the complete carbonyl scrambling occurring in solution for the $[Fe_3(CO)_{11}]^{2-}$ dianion, since these two mechanisms provide no simple pathway for the scrambling of the one face-bridged carbonyl ligand (under the assumption that the limiting low-temperature configuration conforms to that found in the crystalline state).

The Proposed Terminal-Face-Edge Carbonyl Exchange Model for the $[Fe_3(CO)_{11}]^{2-}$ Dianion in Solution and Its Use To Rationalize the Observed Stereodynamic Solution Behavior of the $[HFe_3(CO)_{11}]^-$ Monoanion and of $Ru_3(CO)_{10}(N_2C_4H_4)$. The determined solid-state geometry of the dianion possessing a hitherto unprecedented carbonyl configuration points to a new kind of possible mechanistic pathway for carbonyl interconversion involving a synchronous movement of one axial carbonyl on the unique Fe_A atom with the doubly and triply bridging carbonyl ligands over the two triangular iron faces. This exchange process (Figure 5) may be briefly described as follows. The solid-state C_s $[Fe_3(CO)_{11}]^{2-}$ structure is transformed to an idealized C_{3h} $[Fe_3(CO)_{11}]^{2-}$ structure, which is analogous to the solid-state configuration[27] of $Fe_3(CO)_9(\mu_3\text{-}As)_2$ (vide supra), by concomitant shifts of the doubly bridging and asymmetrical triply bridging carbonyl ligands coupled with rotations of the three terminal carbonyl ligands of each iron atom about its localized threefold axis to minimize steric effects. This C_{3h} structure can be reconverted into the solid-state C_s structure by a reversal of the carbonyl motion, but since the three iron atoms are equivalent under C_{3h} symmetry, the reverse pathway is equally probable along all three directions. This process per se gives rise to an exchange of the two bridging carbonyls with each other as well as an exchange of the basal and axial carbonyl ligands at each iron atom. However, if the carbonyl movement from the C_{3h} to the C_s structure continues in a cyclic process, an interconversion of an axial carbonyl ligand on Fe_A with the triply bridging ligand may be envisioned as follows. (1) The triply bridging carbonyl shifts toward Fe_A, making the bridge more unsymmetrical with the result that it becomes an axial terminal carbonyl of Fe_A. (2) The previous axial carbonyl ligand $CO_{ax(u)}$, located on the same triiron side as the doubly bridging carbonyl and trans to the previously triply bridging carbonyl, bends toward the two basal Fe_B atoms such that it thereby becomes the unsymmetrical triply bridging carbonyl. (3) The doubly bridging carbonyl is flipped from one side of the triiron plane to the other side so that it becomes trans to the new triply bridging carbonyl but cis to the new axial carbonyl. These steps are presumed to take place in a concerted and continuous manner such that at any one time there is at least one triply bridging carbonyl of varying degree of asymmetry to the three iron atoms. This mechanism (Figure 5) enables all of the carbonyl ligands in the dianion to be exchanged as illustrated by the following stages: face-bridged(+) → axial(+) → equatorial → axial(−) → face-bridged(−) → edge-bridged(−) → edge-bridged(+) → face-bridged(+). (Note that the + and − signs differentiate between the two sides of the iron triangle.)

This mechanistic pathway is based upon the following considerations. (1) At any stage of the process, the coordination numbers of the iron atoms do not differ appreciably from those in the static solid-state structure. In particular, negative charge considerations support the premise that any interconversion maintain at least one if not two multiple bridged carbonyl ligands. (2) At any one time in solution, the $[Fe_3(CO)_{11}]^{2-}$ dianions may span a full range of varying degrees of asymmetry of the two bridging carbonyls. Further IR data (vide supra) are needed to clarify this possibility. (3) The proposed edge-face carbonyl movement and bridge-flipping motion of the doubly bridging carbonyl from an upper edge position to a lower one have precedent in the proposed mechanism by Lawson and Shapley[67] for carbonyl exchange in the C_s isomer of $Rh_3(\eta^5\text{-}C_5H_5)_3(CO)_3$.

On the basis of the above scheme, it is also not inconceivable that in the $[HFe_3(CO)_{11}]^-$ monoanion the environments of the doubly bridging carbonyl and one of the axial carbonyl ligands on Fe_A may likewise be selectively averaged (as indicated by the low-temperature ^{13}C NMR data[51]) by a direct synchronous interconversion of the doubly bridging carbonyl and the axial carbonyl on the opposite triiron side in an oscillatory process through a face-bridged intermediate structure with the bridging hydrogen atom concomitantly flipping from one side of the triiron plane to the other side.

Similarly, this proposed mechanism of one axial carbonyl moving directly over a face of the trimetal plane to become a doubly bridging ligand with the other two metal atoms can be used to rationalize part of the observed stereodynamic behavior determined by Cotton et al.[63] for (1,2-diazine)decacarbonyltriruthenium, $Ru_3(CO)_{10}(N_2C_4H_4)$. Its determined molecular structure (Figure 6a) of pseudo C_s-m symmetry may be regarded as a derivative of $Ru_3(CO)_{12}$ in which two cis axial carbonyl ligands on two ruthenium atoms are replaced by the bidentate 1,2-diazine ligand and the six equatorial (in-plane) terminal

(65) Heaton, B. T.; Towl, A. D. C.; Chini, P.; Fumagalli, A.; McCaffrey, D. J. A.; Martinengo, S. *J. Chem. Soc., Chem. Commun.* **1975**, 523–4.
(66) Corey, E. R.; Dahl, L. F.; Beck, W. *J. Am. Chem. Soc.* **1963**, 85, 1202–3.
(67) Lawson, R. J.; Shapley, J. R. *Inorg. Chem.* **1978**, 17, 772–4.

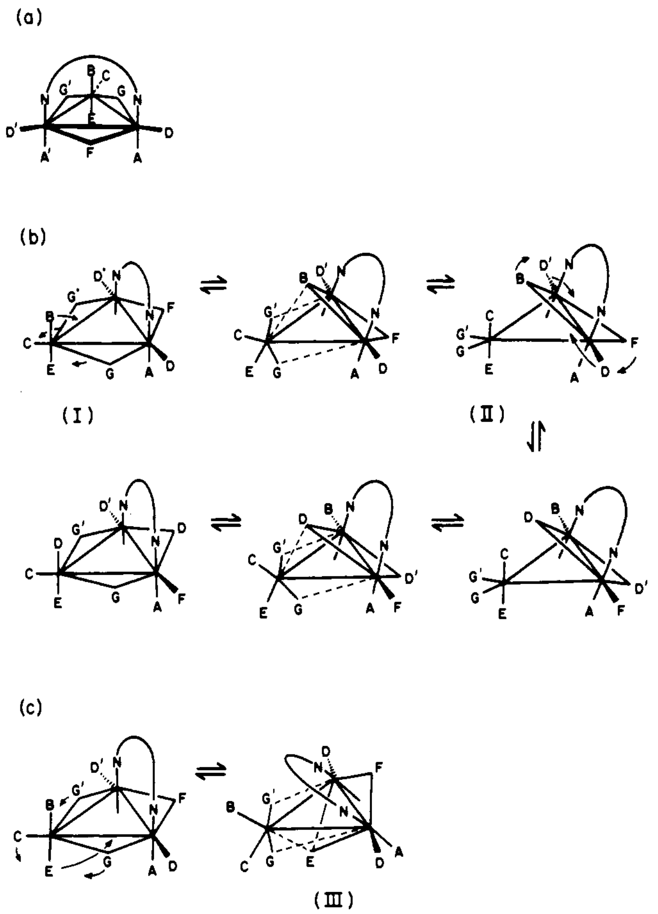

Figure 6. Schematic diagrams showing the following. (a) A representation of the pseudo C_s-m configuration of the $Ru_3(CO)_{10}(N_2C_4H_4)$ molecule with the same carbonyl labeling as that utilized by Cotton and co-workers[63] to describe their proposed assignment of the ^{13}C NMR spectra between −156 °C and +75 °C; (b) our mechanism for the second phase of the three distinct phases of fluxionality (described by Cotton et al.[63]). This second phase is attributed by Cotton et al.[63] to the introduction of one of the two axial carbonyls (either B or E) on the unique Ru atom into the averaging process of six equatorial carbonyls observed in the lower temperature first phase. We suggest that this second phase may be ascribed to a combination of terminal–face–edge exchange and two-center exchange, by which the terminal axial carbonyl B (which is cis to the $N_2C_4H_4$ ligand) enters into the scrambling process. (c) An alternative second-phase mechanism (viewed as sterically *unfavorable* with respect to the one given in (b)), by which a transformation of the other terminal axial carbonyl E into a bridging carbonyl results in an inward tilting of the $N_2C_4H_4$ ligand toward the other bridging ligands G and G′.

carbonyl ligands are rearranged into three terminal and three bridging ones. From a ^{13}C NMR study over the temperature range −156 to +75 °C, Cotton and co-workers[63] observed three distinct phases by which the limiting seven-line slow-exchange spectrum at −156 °C is transformed into a one-line spectrum at +75 °C. Cotton et al.[63] were able to provide a well-defined pathway for the first phase (which consists of scrambling the six equatorial carbonyl ligands) between −156 and ca. −90 °C. However, for the second phase (by which one of the two axial carbonyl ligands B or E joins the rapid in-plane carbonyl scrambling of the first phase) between ca. −115 and −80 °C and for the third phase (which consists of complete scrambling of the carbonyl ligands over all seven structurally different sites) above ca. −30 °C, they pointed out that "there is simply no basis on which to choose any particular process—or processes—for exchanging axial and equatorial CO groups". Hence, they took the position that either of the two carbonyl ligands (B or E) could be involved in the second phase of scrambling.

By the use of a direct axial-to-(face-bridged) carbonyl pathway proposed herein, we believe that a reasonable account of this second-stage fluxional process is possible. As shown in Figure 6b, the axial carbonyl B cis to the $N_2C_4H_4$ bridging ligand moves over the triruthenium plane toward the basal ruthenium atoms through the triply bridging position to become a doubly bridging carbonyl, while at the same time the two bridging carbonyls (G and G′) move in the opposite direction to become terminal carbonyls at the apical ruthenium atom. At this intermediate configuration II, carbonyls B, D, D′, and F are approximately coplanar such that a two-center pairwise-exchange mechanism is possible. A simple pathway is thereby provided for carbonyl B to enter into the triruthenium plane to exchange with the six (originally coplanar) carbonyls (C, D, D′, F, G, and G′). It is also important to note that this mechanism specifically assigns carbonyl B as the axial ligand which enters into the scrambling process between −115 and −80 °C, while the other axial carbonyl E is not exchanging. This conclusion is based upon the premise (Figure 6c) that if the axial carbonyl E forms the bridging carbonyl via our proposed mechanism, the chelating $N_2C_4H_4$ ligand would be required to tilt inward toward the apical ruthenium atom thereby bringing the C_4H_4 substituent too close to the triruthenium plane. The resulting configuration III is considered to be sterically hindered and hence unfavorable relative to the configurations given in Figure 6b.

In conclusion, our proposed pathway for carbonyl scrambling indicates for the first time that a terminal carbonyl can move directly from an axial position to a triply bridging position over the face of a triangle of metal atoms. However, this new mechanism does not negate or exclude the pairwise-exchange mechanism for the $[Fe_3(CO)_{11}]^{2-}$ dianion. In fact, both mechanisms may operate simultaneously. The axial-to-(triply bridging) mechanism proposed here involves more carbonyl ligands in synchronous movement than the pairwise-exchange mechanism and is therefore assumed to be affected more by steric hindrance. For example, in both the $[HFe_3(CO)_{11}]^-$ monoanion and $Ru_3(CO)_{10}(N_2C_4H_4)$, the coordination sites surrounding the three triangular metal atoms are relatively crowded, and hence the pairwise-exchange mechanism occurs at a lower temperature than our proposed axial-to-(triply bridging) mechanism. On the other hand, the coordination environment surrounding the three metal atoms is less crowded in the $[Fe_3(CO)_{11}]^{2-}$ dianion, and hence the axial-to-(triply bridging) mechanism may possibly occur at a lower temperature than that for the pairwise-exchange mechanism.

Acknowledgment. This continuing cooperative research between two universities in Italy and the United States was supported by the National Science Foundation (Grant CHE77-24309). An earlier part of the work was made possible by a joint NATO grant to P.C. and L.F.D.

Supplementary Material Available: A listing of the observed and calculated structure factors (8 pages). Ordering information is given on any current masthead page.